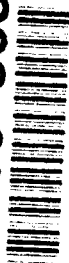


AD-A265 868



NAVAL POSTGRADUATE SCHOOL
Monterey, California



DTIC
ELECTE
MAY 05 1993
S B D

THESIS

A PARAMETRIC ANALYSIS OF ENDOATMOSPHERIC
LOW-EARTH-ORBIT MAINTENANCE

by

Mark S. Wilsey

MARCH 1993

Thesis Advisor:

I.M. Ross

Approved for public release; distribution is unlimited.

93 3 04 01 3

93-09448



Unclassified

Security Classification of this page

REPORT DOCUMENTATION PAGE

1a Source Security Classification: Unclassified		1b Restrictive Markings	
2a Security Classification Authority		3 Distribution Availability: 1 Report	
3a Classification Declassification Schedule		Approved for public release; distribution is unlimited	
4a Funding Organization Report Number(s)		5 Monitoring Organization Report Number(s)	
6a Name of Funding Organization Naval Postgraduate School	6b Office Symbol NPS	7a Name of Monitoring Organization Naval Postgraduate School	
6c Address (city, state, and ZIP code) Monterey, CA 93943-5000		7b Address (city, state, and ZIP code) Monterey, CA 93943-5000	
8a Name of Funding Sponsoring Organization	8b Office Symbol (if applicable)	9 Procurement Instrument Identification Number	
10 Source of Funding Numbers		Program Element No. Project No. Task No. Work Unit Accession No.	

11 Title (include security classification): A PARAMETRIC ANALYSIS OF ENDOATMOSPHERIC LOW-EARTH-ORBIT MAINTENANCE

12 Personal Author(s): Wilsey, Mark S.

13a Type of Report Master's Thesis	13b Time Covered From To	14 Date of Report (year, month, day) March 1993	15 Page Count 83
---------------------------------------	-----------------------------	----------------------------------------------------	---------------------

16 Supplementary Notation: The views expressed in this thesis are those of the author and do not reflect the official policy or position of the Department of Defense or the U.S. Government.

17a Subject Codes			18 Subject Terms (continue on reverse if necessary and identify by block number) orbits, low-Earth orbiting, satellites, orbital maintenance, fuel optimization
Field	Group	Subgroup	

19 Abstract (continue on reverse if necessary and identify by block number)

With the advent of long term low Earth-orbiting satellites comes the requirement to maintain a specified orbital radial band. Optimal control theory suggests that periodic thrusting is more efficient than forced Keplerian motion in orbital maintenance through the use of Primer vectoring. This thesis examined the efficiency of fixed-angle transverse thrusting as an alternative to Primer vectoring. Numerical analysis shows that a thrust angle of 65-70 degrees is feasible for radial band control for a wide range of parameters. Fuel usage can be minimized through the proper selection of radial bandwidth, thruster size, and thrust angle. This thesis shows that forced Keplerian motion is always superior to fixed-angle transverse thrusting from a fuel usage standpoint, and hence that thrust vectoring must be utilized.

20 Distribution/Availability of Abstract __ unclassified/unlimited __ same as report __ DTIC users		21 Abstract Security Classification Unclassified	
22a Name of Responsible Individual I.M. Ross		22b Telephone (include Area Code) (408) 656-2074	22c Office Symbol AA/Ro

Approved for public release; distribution is unlimited.

A Parametric Analysis of Endoatmospheric
Low-Earth-Orbit Maintenance

by

Mark S. Wilsey
Lieutenant Commander, United States Navy
B.S., United States Naval Academy, 1979

Submitted in partial fulfillment
of the requirements for the degree of

MASTER OF SCIENCE IN ASTRONAUTICAL ENGINEERING

from the

NAVAL POSTGRADUATE SCHOOL
March 1993

Author:

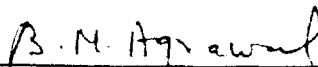


Mark S. Wilsey

Approved by:



I.M. Ross, Thesis Advisor



Brij Agrawal, Second Reader



Daniel J. Collins, Chairman

Department of Aeronautics and Astronautics

ABSTRACT

With the advent of long term low Earth-orbiting satellites comes the requirement to maintain a specified orbital radial band. Optimal control theory suggests that periodic thrusting is more efficient than forced Keplerian motion in orbital maintenance through the use of Primer vectoring. This thesis examined the efficiency of fixed-angle transverse thrusting as an alternative to Primer vectoring. Numerical analysis shows that a thrust angle of 65-70 degrees is feasible for radial band control for a wide range of parameters. Fuel usage can be minimized through the proper selection of radial bandwidth, thruster size, and thrust angle. This thesis shows that forced Keplerian motion is always superior to fixed-angle transverse thrusting from a fuel usage standpoint, and hence that thrust vectoring must be utilized.

Accession For	
NTIS	<input checked="" type="checkbox"/>
DTIC TAB	<input type="checkbox"/>
Unannounced	<input type="checkbox"/>
Justification	
By	
Distribution/	
Availability Codes	
Avail and/or	
Dist	Special
A-1	

TABLE OF CONTENTS

I.	INTRODUCTION	1
II.	GENERAL FORMULATION OF THE PROBLEM	2
III.	FORMULA DEVELOPMENT	3
	A. DEVELOPMENT OF THE EQUATIONS OF MOTION	3
	B. NONDIMENSIONALIZATION OF THE EQUATIONS OF MOTION	4
	1. Definitions	4
	2. Nondimensionalization	7
	C. NONDIMENSIONALIZATION OF ATMOSPHERIC DRAG	10
	1. Definitions	10
	2. Nondimensionalization	10
	D. DEVELOPMENT OF MASS EQUATIONS	13
IV.	DEVELOPMENT AND VALIDATION OF COMPUTER MODEL	14
	A. COMPUTER PROGRAM DEVELOPMENT	14
	B. PROGRAM VALIDATION	16
	1. Initial validation with no external forces	16
	2. Validation of drag	16
	3. Validation of thrust	20
	C. ORBIT CONTROL STRATEGY	20
	1. Control using radius	21
	2. Control using total energy	22
	3. Control using radius and total energy	22

4. Control using specific energy	41
5. Control using radius and specific energy	42
V. ANALYSIS AND RESULTS	43
A. VARIATION OF THRUST ANGLE, θ	43
B. VARIATION OF PRE-SPECIFIED RADIAL BANDWIDTH	47
C. VARIATION OF ATMOSPHERIC SCALE HEIGHT, h_0	49
D. VARIATION OF THRUST, T	49
E. VARIATIONS IN NONDIMENSIONALIZED BALLISTIC COEFFICIENT	42
VI. CONCLUSIONS AND RECOMMENDATIONS	46
APPENDIX A	48
A. PROGRAM LISTING	48
B. SAMPLE INPUT FILE	47
C. SAMPLE OUTPUT FILE	47
APPENDIX B	50
APPENDIX C	54
APPENDIX D	59
APPENDIX E	63
APPENDIX F	67
APPENDIX G	69
APPENDIX H	71
LIST OF REFERENCES	75
INITIAL DISTRIBUTION LIST	76

I. INTRODUCTION

Orbital maintenance for low-Earth orbiting (LEO) satellites can be accomplished using forced Keplerian motion or by bang-bang control. Forced Keplerian motion utilizes constant thrust, with magnitude equal to drag, to prevent orbital decay and maintain orbital altitude. Bang-bang control allows the satellite orbit to decay and then fires thrusters to reboost the satellite and keep it within a prescribed radial band. This can be modeled as a series of orbital transfers offsetting decay due to atmospheric drag. Currently, LEO satellites are not required to maintain a specified orbital band, and are reboosted only to prevent reentry or to change orbit.

Historically, co-planar orbital transfers have been optimally accomplished using two or three-impulse Hohmann maneuvers [Ref. 1:pp 78-88]. These maneuvers are designed for one-time transfers between exo-atmospheric orbits, not for a series of maneuvers to offset drag and maintain an orbital band. Bang-bang control utilizes one thruster firing per reboost of the satellite, vice two or three firings used in a Hohmann transfer.

In Ref. 2, the problem of minimum-fuel orbital maintenance for low-altitude, non-lifting bodies was considered, with the conclusion that fixed-angle, transverse

thrusting (i.e. bang-bang control with the thrust vector at a constant angle relative to the local horizontal, is less efficient than forced Keplerian motion. This topic was first explored by Ross and Melton [Ref. 3] who concluded that forced Keplerian motion is not the optimal solution for this problem. Development of long-term, low-altitude satellites, such as the space station, dictate continued research into this topic to resolve this apparent contradiction.

Little research has been done on the optimization of bang-bang control in relation to atmospheric effects on non-lifting (blunt) bodies. A better understanding of these effects is essential for optimization of orbits and propulsion equipment for long-term satellites, including the space station. Additionally, design and operation of lifting bodies may benefit from this study.

II. GENERAL FORMULATION OF THE PROBLEM

Two methods of optimizing orbital transfers for LEO satellites have been studied in Ref. 2 and Ref. 3. On the basis of numerical simulations, Pauls [Ref. 2] concludes that bang-bang control is less efficient than forced Keplerian motion, and that transverse thrusting at a fixed angle of 70 degrees is generally the optimal feasible solution for orbital maintenance if bang-bang control is used. This apparently contradicts the analytical results of Ross and Melton [Ref. 3], who conclude that forced Keplerian motion is not optimal and that a bang-bang solution exists that optimizes fuel usage. This leads Pauls to conclude that variable thrust-vectoring is essential for optimality during finite-burns. However, Pauls study was limited to a small class of satellites (essentially space platforms) in the upper atmosphere. Therefore, his conclusions are not globally valid, and questions remain. Is transverse thrusting less efficient than forced Keplerian motion for all parameters? What exactly are these parameters? Is the 70 degree thrust angle always optimal? This thesis will try to answer some of these questions.

The problem is defined as maintaining a spacecraft within a prescribed radial band $R_{\min} \leq R \leq R_{\max}$. Comparison of

fuel usage for bang-bang control and forced Keplerian motion, over a wide range of parameters, will provide insights on the optimality question. Also, determination of a thrust angle, or range of angles, that optimizes the bang-bang control solution is desired.

Ross and Melton [Ref. 3] base their conclusions on methods utilizing optimal control theory, which require initial and boundary conditions to facilitate a solution using numerical integration. This is a cumbersome solution technique that requires recomputation for slight changes in initial or boundary conditions. While this may be the most accurate solution technique, it is not easy or very practical.

Pauls [Ref. 2] develops a computer model to solve this problem. Equations of motion were derived and solved for various parameter combinations to optimize bang-bang control. Attempts to define a radial band and then control the spacecraft within that band were unsuccessful. However, maintaining specific energy allowed a band to be maintained, albeit larger than the desired band. All solutions to this model predicted that forced Keplerian motion is more efficient than bang-bang control.

Further study using a computer model is dictated. Non-dimensionalization of the equations of motion will allow effects of variations in parameters to be more easily analyzed. Variations of parameters will be analyzed for

trends and effects on solutions, leading to optimal solutions for design of bang-bang control systems such as thruster size, thrust angle, and size of radial band. Optimality will be based on fuel usage, maintenance of the required radial band with minimal eccentricity, and thruster firing patterns. An ability to predict the actual radial band controlled is desired.

Results of the computer model will then be compared to those obtained using forced Keplerian motion to determine the optimal means of maintaining a spacecraft within a design radial band while subjected to continuous atmospheric drag.

III. FORMULA DEVELOPMENT

A. DEVELOPMENT OF THE EQUATIONS OF MOTION

For simplification, orbital motion is assumed to be coplanar and initially circular. Assuming a non-lifting blunt body, drag becomes the only aerodynamic force perturbing the orbit and thrust is the external force applied to counter-balance drag. The external forces acting on the spacecraft consist of gravity, aerodynamic drag, and thrust. Figure 1 shows the coordinate system and net forces for this two-body problem.

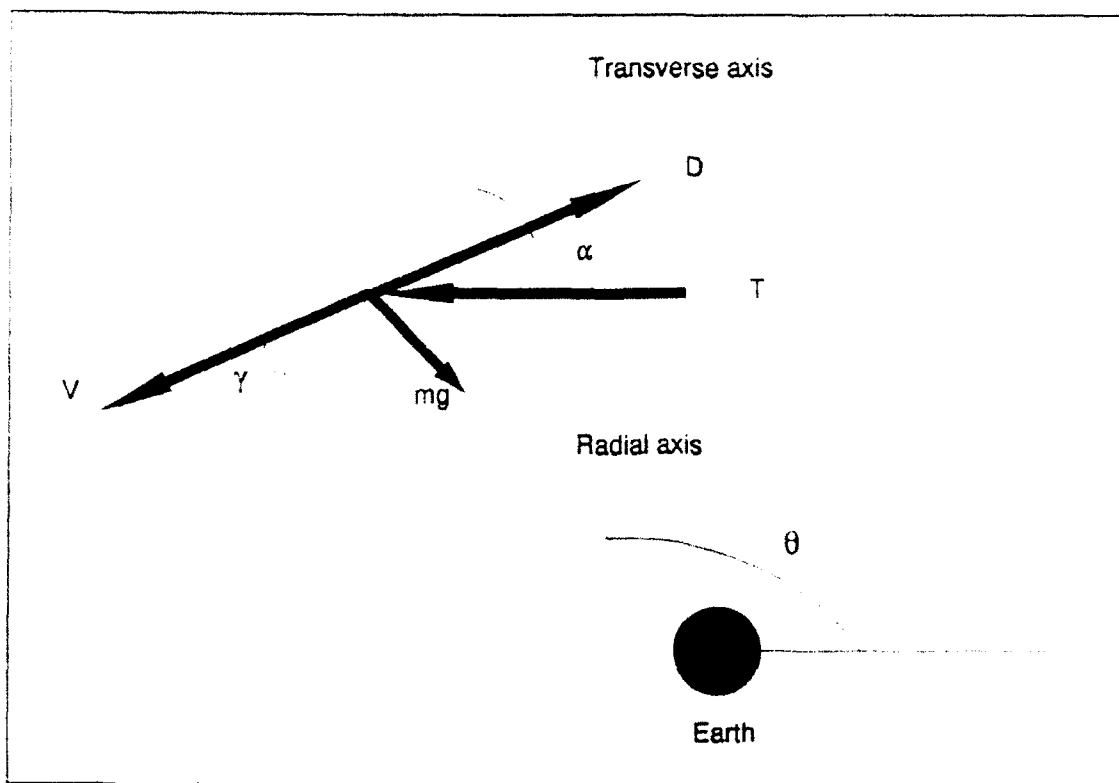


Figure 1 Graphical Representation of Coordinate System

The equations of motion for this two-body problem are

$$\ddot{r} = -\frac{\mu}{r^2} + \frac{\Sigma F_r}{m} \quad (1)$$

$$r\ddot{\theta} + 2\dot{r}\dot{\theta} = \frac{\Sigma F_\theta}{m} \quad (2)$$

where a_r and a_θ are the radial and transverse accelerations and ΣF_r and ΣF_θ are the sums of the external radial and transverse forces, respectively, and m is spacecraft mass. From Figure 1, the components of drag are

$$D_r = -D \sin(\gamma) \quad (3)$$

$$D_\theta = -D \cos(\gamma) \quad (4)$$

and the components of thrust are

$$T_r = T \sin(\alpha) \quad (5)$$

$$T_\theta = T \cos(\alpha) \quad (6)$$

The angle γ is the flight path angle and is defined by the intersection of the velocity vector and transverse axis, while angle α is the thrust angle and is defined by the intersection of the thrust vector and transverse axis. The equations of motion can now be written

$$r'' - \theta'^2 r = -\frac{\mu}{r^2} - \frac{D_r}{m} + \frac{T_r}{m} \quad (7)$$

$$\theta'' r + 2\theta' r' = -\frac{D_\theta}{m} + \frac{T_\theta}{m} \quad (8)$$

where μ is the Earth's gravitational constant, θ is the angular position of the spacecraft, and primes denote differentiation with respect to time.

B. NONDIMENSIONALIZATION OF THE EQUATIONS OF MOTION

The equations of motion are nondimensionalized so that variations in parameters are minimized. The nondimensionalizing constants are chosen to "balance" the equations and thus produce the same order of magnitude responses. This facilitates study of the effects of changing parameters on the optimization problem.

1. Definitions

In order to nondimensionalize the equations, variables must be defined and nondimensionalizing constants must be chosen. Nondimensionalizing constants for radius and time are designated R and τ , respectively, and were chosen somewhat arbitrarily based on the Earth's radius. Thus, R is the radius of the Earth and τ is the period of a circular orbit whose radius equals R , and is defined as

$$\tau = 2\pi \sqrt{\frac{R^3}{\mu}} \quad (9)$$

These constants define the nondimensionalized variables for radius and time

$$\bar{r} = \frac{r}{R} \quad (10)$$

$$\bar{t} = \frac{t}{\tau} \quad (11)$$

The nondimensionalizing factor for mass is M (spacecraft initial mass), which defines the nondimensionalized mass

$$\bar{m} = \frac{m}{M} \quad (12)$$

The variable θ is already dimensionless.

2. Nondimensionalization

Using the above definitions, the following relationships are developed.

$$\frac{d\bar{r}}{d\bar{t}} = \frac{\tau}{R} \frac{dr}{dt} \quad (13)$$

$$\frac{d^2\bar{r}}{d\bar{t}^2} = \frac{d}{d\bar{t}} \left(\frac{\tau}{R} \frac{dr}{dt} \right) = \frac{\tau^2}{R} \frac{d^2r}{dt^2} \quad (14)$$

$$\frac{d\theta}{d\bar{t}} = \tau \frac{d\theta}{dt} \quad (15)$$

$$\frac{d^2\theta}{d\bar{t}^2} = \frac{d}{d\bar{t}} \left(\tau \frac{d\theta}{dt} \right) = \tau^2 \frac{d^2\theta}{dt^2} \quad (16)$$

Substituting these equations into the equations 7 and 8, substituting equation 9 for τ where convenient, and

rearranging terms, yields the following nondimensionalized results

$$\frac{d^2\bar{r}}{d\bar{t}^2} = \bar{r} \left(\frac{d\theta}{d\bar{t}} \right)^2 - \frac{4\pi^2}{\bar{r}^2} - \frac{\bar{r}^2}{R} \frac{D \sin \gamma}{\bar{M}} + \frac{\bar{r}^2}{R} \frac{T \sin \alpha}{\bar{M}} \quad (17)$$

$$\frac{d^2\theta}{d\bar{t}^2} = -\frac{2}{\bar{r}} \frac{d\theta d\bar{r}}{d\bar{t}^2} - \frac{\bar{r}^2}{R\bar{r}} \frac{D \cos \gamma}{\bar{M}} + \frac{\bar{r}^2}{R\bar{r}} \frac{T \cos \alpha}{\bar{M}} \quad (18)$$

C. NONDIMENSIONALIZATION OF ATMOSPHERIC DRAG

1. Definitions

Drag is given by

$$D = \frac{1}{2} \rho S_{ref} C_d V^2 \quad (19)$$

where ρ is atmospheric density (altitude dependent), S_{ref} is the reference surface area of the spacecraft affected by atmospheric density, C_d is the coefficient of drag, and v is spacecraft velocity.

2. Nondimensionalization

Nondimensionalization of v^2 is accomplished using the relationship

$$v^2 = \dot{r}^2 + r^2 \dot{\theta}^2 = \left(\frac{dr}{d\bar{t}} \right)^2 + r^2 \left(\frac{d\theta}{d\bar{t}} \right)^2 \quad (20)$$

Substituting equations 10, 13, and 15 gives

$$\dot{V}^2 = \frac{R^2}{\tau^2} \left[\left(\frac{d\bar{F}}{d\bar{t}} \right)^2 + \bar{F}^2 \left(\frac{d\theta}{d\bar{t}} \right)^2 \right] = \frac{R^2}{\tau^2} \bar{V}^2 \quad (21)$$

which is then substituted into equation 19 and simplified into the form used in equations 17 and 18 to give

$$\frac{\tau^2}{R} \frac{D}{\bar{M}} = \frac{\tau^2}{R} \frac{\rho S_{ref} C_D R^2 \bar{V}^2}{2 \bar{M} \tau^2} = \frac{\rho R \bar{V}^2}{2 \bar{M} B} \quad (22)$$

where B is the initial ballistic coefficient and defined as

$$B = \frac{M}{C_D S_{ref}} \quad (23)$$

This result is then put back into equations 17 and 18 to yield the nondimensionalized equations

$$\frac{d^2 \bar{F}}{d\bar{t}^2} = \bar{F} \left(\frac{d\theta}{d\bar{t}} \right)^2 - \frac{4\pi^2}{\bar{F}^2} - \frac{\rho R \bar{V}^2 \sin \gamma}{2 \bar{M} B} + \frac{\tau^2}{R} \frac{T \sin \alpha}{\bar{M}} \quad (24)$$

$$\frac{d^2 \theta}{d\bar{t}^2} = -\frac{2}{\bar{F}} \frac{d\theta d\bar{F}}{d\bar{t} d\bar{t}} - \frac{\rho R \bar{V}^2 \cos \gamma}{2 \bar{M} B \bar{F}} + \frac{\tau^2}{R \bar{F}} \frac{T \cos \alpha}{\bar{M}} \quad (25)$$

Inspection of these equations reveals that further simplification is possible. Assuming an exponential atmospheric density model (which will be used throughout the study of this problem), with atmospheric scale height β defines

$$\rho = \rho_0 e^{-\beta(x-R_{ref})} \quad (26)$$

This allows the ballistic coefficient, B, to be nondimensionalized as

$$\bar{B} = \frac{B}{\rho_0 R} \quad (27)$$

The thrust terms can be similarly nondimensionalized by defining a nondimensionalized thrust

$$\bar{T} = \frac{T}{MR} \quad (28)$$

Substituting equations 27 and 28 into equations 24 and 25, and nondimensionalizing the exponent for drag result in the final equations

$$\frac{d^2 \bar{r}}{d\bar{t}^2} = \bar{r} \left(\frac{d\theta}{d\bar{t}} \right)^2 - \frac{4\pi^2}{\bar{r}^2} - \frac{e^{-\beta R(\bar{r} - \frac{R_{ref}}{R})} \bar{r}^2 \sin \gamma}{2m\bar{r}\bar{B}} - \frac{\bar{T} \sin \alpha}{\bar{m}} \quad (29)$$

$$\frac{d^2 \theta}{d\bar{t}^2} = -\frac{2}{\bar{r}} \frac{d\theta d\bar{r}}{d\bar{t} d\bar{t}} - \frac{e^{-\beta R(\bar{r} - \frac{R_{ref}}{R})} \bar{r}^2 \cos \gamma}{2m\bar{r}\bar{B}} + \frac{\bar{T} \cos \alpha}{m\bar{r}} \quad (30)$$

These equations will be used to generate the computer model to study the optimality problem of bang-bang control. The only parameters that need to be varied to study the optimality problem are

$$\alpha, \beta, \bar{T}, \bar{B}$$

Since the only variable parameter in the nondimensionalized thrust term is thrust, T , either one can be varied for the study.

D. DEVELOPMENT OF MASS EQUATIONS

One of the optimality criteria to be used in this study is the mass of fuel consumed to maintain orbit. The relationship

$$\dot{m} = \frac{dm}{dt} = -\frac{T}{c_{sp}g} \quad (31)$$

defines the rate of fuel consumption and can be integrated over time to determine the total fuel consumed. Using equations 11, 12, and 29, this can be nondimensionalized and simplified to

$$\frac{d\bar{m}}{d\bar{t}} = -\frac{R}{\gamma} \frac{\bar{T}}{c_{sp}g} \quad (32)$$

These equations will be used to calculate the fuel used to maintain orbit using bang-bang control for comparison to fuel used in forced Keplerian motion.

IV. DEVELOPMENT AND VALIDATION OF COMPUTER MODEL

A. COMPUTER PROGRAM DEVELOPMENT

A computer program, written in FORTRAN and listed in Appendix A with sample input and output files, was developed to simulate spacecraft orbital motion. A fourth-order Runge-Kutta numerical integration routine is used to integrate the equations of motion. The program is comprised of a main program section, which controls input, output, and flow of information, and five subroutines that provide computations necessary to simulate orbital motion and calculate the osculating orbital parameters.

The non-dimensionalized equations previously developed (equations 29 and 30) are simplified for use in the computer program using the following state variable definitions.

$$x_1 = r \quad (33)$$

$$x_2 = \frac{dx_1}{dt} = \frac{dr}{dt} \quad (34)$$

$$x_3 = \theta \quad (35)$$

$$x_4 = \frac{dx_3}{dt} = \frac{d\theta}{dt} \quad (36)$$

These state variables are nondimensionalized as follows

$$\overline{X_1} = \frac{r}{R} = \frac{X_1}{R} = \overline{r} \quad (37)$$

$$\overline{X_2} = \frac{d\overline{r}}{d\overline{t}} = \frac{1}{R} \frac{dr}{dt} = \frac{1}{R} \dot{r} \quad (38)$$

$$\overline{X_4} = \frac{d\theta}{d\overline{t}} = \tau \frac{d\theta}{dt} = \tau \dot{\theta} = \overline{\omega} \quad (39)$$

The state variable x_1 is already nondimensionalized. These equations are then substituted into equations 29 and 30 to give the equations of motion used in the computer program.

$$\frac{d\overline{X_2}}{d\overline{t}} = \overline{X_1 X_4} - \frac{4\pi^2}{\overline{X_1^2}} - \frac{e^{-jR(\overline{t} - \frac{R_{c1}}{R})} \overline{V}^2 \sin \gamma}{2\overline{m}B} + \frac{T \sin \alpha}{\overline{m}} \quad (40)$$

$$\frac{d\overline{X_4}}{d\overline{t}} = -\frac{2}{\overline{X_1}} \overline{X_1 X_2} - \frac{e^{-jR(\overline{t} - \frac{R_{c1}}{R})} \overline{V}^2 \cos \gamma}{2\overline{m}RB} + \frac{T \cos \alpha}{\overline{m}R} \quad (41)$$

The first subroutine, DRAG, calculates the atmospheric drag experienced by the spacecraft. A constant atmospheric density model is used for initial program validation, after which an exponential density model is used. The second subroutine, EQN, updates the equations of motion that define the spacecraft's orbital motion, equations 40 and 41. The third subroutine, ORBPARG, calculates the osculating orbital parameters for the spacecraft's motion, including semi-major axis, apogee, perigee, and period. The fourth subroutine, RK4, is a standard fourth-order Runge-Kutta numerical

integration routine that integrates the state variables. The last subroutine, THRUST, governs the activation and deactivation of the thrusters to maintain the satellite's orbit.

B. PROGRAM VALIDATION

1. Initial validation with no external forces

Program validation proceeded in a logical series of steps, with each step requiring positive validation before proceeding to the next step. Initially, all external forces except gravity were neglected in order to maintain a circular orbit. As shown in Appendix B, Figures 1-4, radius, velocity, angular momentum, and specific energy all remained constant. Initial conditions of an elliptic orbit were then input into the program with all external forces except gravity neglected. Figures 5-8 of Appendix B show that semi-major axis (SMA), eccentricity, specific energy and angular momentum are constant. This validates the initial program.

2. Validation of drag

A constant atmospheric density was then introduced into the program, with a value that would produce a noticeable effect in a small number of orbits to enhance the validation process. The program was run for ten orbits and the results compared with analytical results obtained using equations from Ref. 4,

$$\Delta a = -2\pi \left(\frac{C_d S_{ref}}{M} \right) \rho a^2 \quad (42)$$

$$\Delta V = -\pi \left(\frac{C_d S_{ref}}{M} \right) \rho a V \quad (43)$$

$$\Delta P = -6\pi \left(\frac{C_d S_{ref}}{M} \right) \rho \frac{a^3}{V} \quad (44)$$

which show the changes in semi-major axis, velocity, and period per orbit of a spacecraft under drag. In all of these equations, ballistic coefficient (B) was substituted for $M/C_d S_{ref}$. The program was run using both radius and semi-major axis for the term "a" in the above equations. Results should be very similar since semi-major axis and radius are assumed to be equal in the formulation of the analytic equations and should be relatively equal for the small changes expected. Percent errors were calculated for the computed vs analytical results for changes in semi-major axis (SMA), velocity (VEL), and period (PER), as well as for the percent differences between computed and analytical values of semi-major axis, velocity, and period after each orbit. Table I shows the results when radius is used in the analytical equations for "a", while Table II shows the results when semi-major axis is used in the analytical equations for "a". As shown in Table I, the percent error for the changes in semi-major axis (%ΔSMA error) and period (%ΔPER error) start small after one orbit, grow through the

Table I COMPUTED AND ANALYTIC ERRORS USING RADIUS

ORBIT #	% Δ SMA ERROR	%SMA ERROR	% Δ P ERROR	% PER ERROR	% Δ V ERROR	% VEL ERROR
1	0.4317	.00001	0.4318	.00000	7.2875	.00015
2	1.6709	.00003	1.6710	.00001	5.1534	.00029
3	3.5508	.00004	3.5509	.00002	1.8283	.00043
4	5.8015	.00005	5.8017	.00005	2.2979	.00056
5	8.0777	.00006	8.0779	.00008	6.6409	.00069
6	10.017	.00007	10.017	.00012	10.484	.00081
7	11.323	.00009	11.326	.00015	13.155	.00094
8	11.860	.00010	11.860	.00018	14.265	.00107
9	11.665	.00011	11.666	.00020	13.859	.00120
10	10.948	.00012	10.948	.00021	12.377	.00134

Table II COMPUTED AND ANALYTIC ERRORS USING SEMI-MAJOR AXIS

ORBIT #	% Δ SMA ERROR	% SMA ERROR	% Δ P ERROR	% PER ERROR	% Δ V ERROR	% VEL ERROR
1	9.5531	.00001	9.5531	.00002	7.2875	.00015
2	9.5531	.00003	9.5532	.00004	5.1534	.00029
3	9.5531	.00004	9.5532	.00006	1.8283	.00043
4	9.5532	.00005	9.5533	.00007	2.2979	.00056
5	9.5532	.00006	9.5534	.00009	6.6409	.00069
6	9.5532	.00007	9.5535	.00011	10.484	.00081
7	9.5533	.00009	9.5535	.00013	13.155	.00094
8	9.5533	.00010	9.5536	.00015	14.265	.00107
9	9.5533	.00011	9.5537	.00017	13.859	.00120
10	9.5534	.00012	9.5537	.00019	12.377	.00134

fifth orbit, and then steady out at roughly eleven percent. This final error percentage closely corresponds to the relatively constant 9.8% error found when using semi-major axis in Table II. However, in both cases, as shown in Tables I and II, the percent error between the calculated and analytic semi-major axis (% SMA error) and period (% PER error) after each orbit is less than 0.0003%. The absolute percent error in the change in velocity (% ΔV error) and the difference between the calculated and analytic velocity (% VEL error) after each orbit are the same whether using semi-major axis or radius for "a", as shown in Tables I and II. Again, while the percent error in the change in velocity grows to greater than ten percent, the percent error between calculated and analytic velocity after each orbit very small (less than 0.002%). The reason for the ten percent errors between parameter changes appears to be the accuracy involved when the changes are so small (i.e. semi-major axis is changing by approximately 200 meters per orbit out of an initial orbit of 6638200 meters). Thus an error of 10% in change of semi-major axis is only 20 meters, which is insignificant in terms of the initial radius. The analytic and computed results are thus in agreement and the drag portion of the program is validated.

3. Validation of thrust

The thrust portion of the program was validated throughout the study by having drag present and the spacecraft maintain an orbital band by reboosting using thrusters.

C. ORBIT CONTROL STRATEGY

It is desired to design a control strategy that is simple and will maintain the spacecraft within a pre-specified radial band. Figure 2 shows a typical band, defining limits of radius and specific energy.

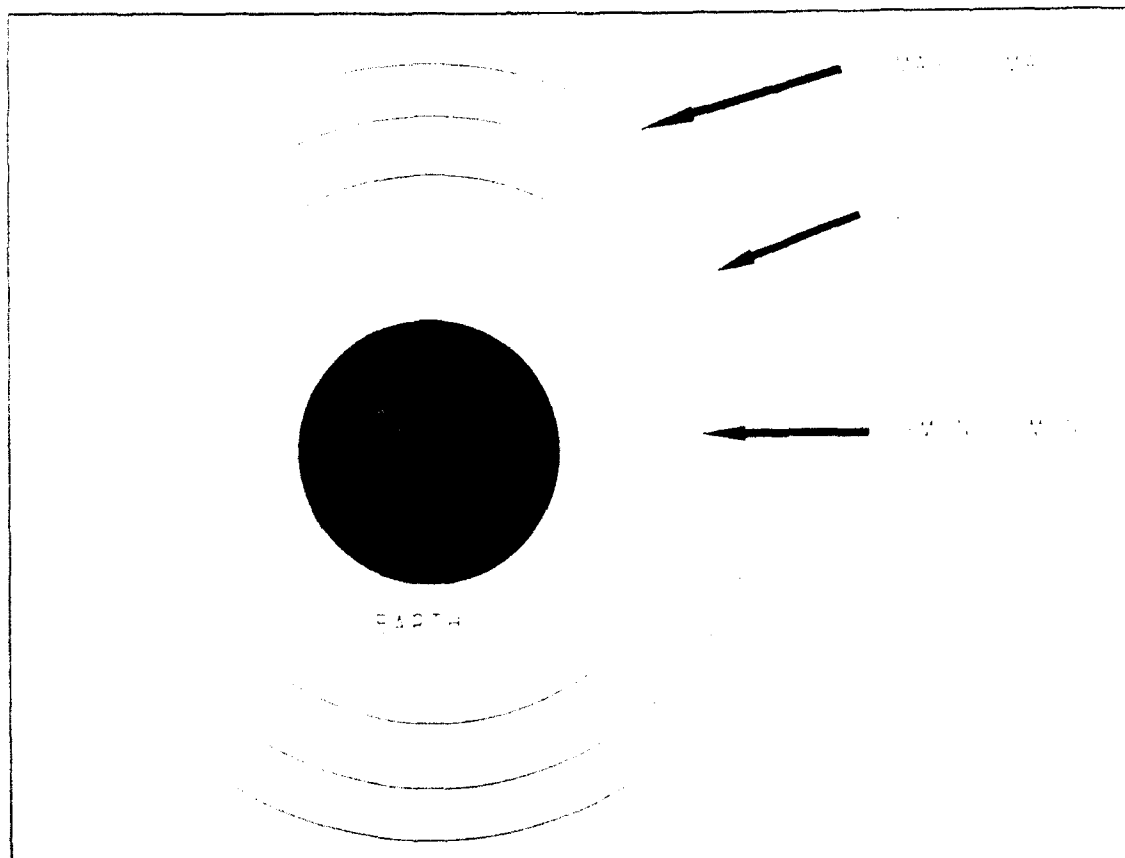


Figure 2 Orbital band with radius and energy

All control strategies were run using numerous combinations of parameter values (i.e. thrust vector angle, α , was varied from 0-90° in 5° increments, radial band was varied using 25, 55 and 100 km bands, thrust was varied from 25 to 300 N., etc.). For consistency, all cases presented here were run with the following baseline values

$R_0 = 6638.2 \text{ km}$
 $M = 20000 \text{ kg}$
 $\text{Thrust} = 300 \text{ N}$
 $\text{Ballistic coefficient} = B = 150 \text{ kg m}^2$
 $\rho_0 = 9.4 \times 10^{-10} \text{ kg m}^{-3}$
 $\beta = 2.12 \times 10^{-5} \text{ km}^{-1}$
 $T_{sp} = 300 \text{ sec}$
 $\alpha = 70^\circ$
 $\text{Radial band} = 2 \text{ km}$

which produce representative results corresponding to

$\bar{E} = 25000$
 $\bar{T} = 0.060$

1. Control using radius

Initial attempts were made to control the radial band using radius as a parameter, i.e. turn thrusters on when the radius drops to the low end of the band (RMIN) and turn them off when the satellite is reboosted to the high end of the band (RMAX). As shown in Figures 1 of Appendix C, this control strategy was ineffective because the specific energy of the orbit continually increased and never leveled off (see Appendix C, Figure 2). The eccentricity of this orbit grew to approximately 0.1.

2. Control using total energy

Control was next attempted using total energy. The total energy of the initial orbit was calculated, as were the total energies of the spacecraft in circular orbits at the minimum and maximum of the radial band (see Figure 2) using

$$E_j = m \left(\frac{V^2}{2} - \frac{\mu}{r} \right) \quad (45)$$

The thrusters were turned on when the spacecraft total energy dropped below the minimum orbit total energy and turned off when the spacecraft total energy rose above maximum orbit total energy. This method failed to control radius, as the spacecraft orbit always eventually decayed, but successfully controlled energy, as shown in Figures 3 and 4 of Appendix C. While this method succeeded in maintaining a pre-determined radial band, the orbital radius was not maintained and decayed.

3. Control using radius and total energy

A combination control strategy utilizing both radius and total energy was attempted. Thrusters were turned on when the orbital radius dropped to the minimum radius and turned off when total energy increased to the initial total energy. Figures 5 and 6 of Appendix C show the unsuccessful results. Total energy would seem to be the parameter of choice for maintaining the orbit vice specific energy.

However, if the total energy is maintained at a constant value the orbital radius must decrease and/or velocity must decrease since the spacecraft mass decreases due to thrusting. This can be shown using equation 13.

4. Control using specific energy

The next attempt at control involved spacecraft specific energy. This control was similar to the attempt using total energy, only specific energy was used. Specific energy is a function of orbital radius (for circular orbits), so "conserving" specific energy should result in a "conservation" of radius (i.e. a constant average radius). As shown in Figure 7 of Appendix C, the orbital radius was maintained, however the orbital band was not. Conserving spacecraft specific energy, as shown in Figure 8 of Appendix C, failed to maintain the initial radius of the spacecraft.

5. Control using radius and specific energy

Control using radius and spacecraft specific energy is successful in maintaining radius and a radial band, as shown in Figures 9 and 10 of Appendix C. Thrusters are turned on based on the spacecraft orbit decaying below a specified radial minimum and spacecraft specific energy being below the initial specific energy. Thrusters remain on until specific energy increases above the initial value. This control strategy results in an orbit whose radius oscillates about the initial radius, but not necessarily at

the pre-specified value. The variation of the actual radial band from the desired band varies and is examined in greater detail in the next chapter.

V. ANALYSIS AND RESULTS

Analysis of the validated control strategy is performed in five steps. A set of parameter values is chosen as the baseline case about which they will be varied. These values are selected as representative of a space-station/platform type satellite. The baseline values are

$$\begin{aligned} R &= 6638.2 \text{ km} \\ M &= 20000 \text{ kg} \\ I_{sp} &= 300 \text{ sec} \\ T &= 300 \text{ N} \\ \rho_0 &= 9.4 \times 10^{-10} \text{ kg/m}^3 \\ B &= 150 \text{ kg/m}^2 \\ \bar{B} &= 25000 \\ \beta &= 2.12 \times 10^{-5} \text{ km}^{-1} \end{aligned}$$

The simulation program is run for 100 orbits, with the equations of motion updated 5000 times per orbit, and output sampled 100 times per orbit.

A. VARIATION OF THRUST ANGLE, α

First, numerous cases are studied to determine the validity of an optimal thrust angle, α , of 70° . The program is run with combinations of variations of parameters about the baseline values, while varying α from $0-90^\circ$ in 5° increments. In all cases, thrust angles of 65 and 70° are the only values that maintain a constant radial band. Figures 1-4 of Appendix D show results over the range of $60-$

75° for the baseline parameters, and are representative of all cases. Values of α below 60° and above 75° produce results that degrade significantly from those shown. Semi-major axis (SMA) and eccentricity are also compared throughout the analysis for determining optimal values of α . Figures 5 and 6 of Appendix D show results consistent with a maintained radial band ($\alpha=70^\circ$), while Figures 7 and 8 show results consistent with a radial band not being maintained ($\alpha=50^\circ$). As can be seen, eccentricity must level off to a constant value to maintain a radial band, while SMA alone is not an indicator of orbital maintenance.

The mass of fuel required to maintain orbit generally increases as α increases from 0 to 90°, with some minor local fluctuations. Table III shows the mass of fuel burned in kilograms (kg) to maintain 2, 25, and 100 km pre-specified bands, with α varying from 60-75° and baseline

Table III MASS OF FUEL BURNED (kg)

Band (km)	$\alpha=60^\circ$	$\alpha=65^\circ$	$\alpha=70^\circ$	$\alpha=75^\circ$
2	2049	2013	2174	2683
25	2643	2828	3243	3595
100	3020	2853	2826	3787

values for other parameters, and is typical of the trend seen. Thus, from a fuel usage standpoint α should be

minimized, but from a radial band standpoint α must be in the range of 65-70°.

This shows that a constant thrust angle, α , of approximately 65-70° is necessary to maintain a radial band. The following analyses are conducted with a range of 60-75° for α to minimize the data collection while ensuring the continuing validity of this result.

B. VARIATION OF PRE-SPECIFIED RADIAL BANDWIDTH

Once α is chosen, it is desired to know how the pre-specified radial bandwidth affects the results. While maintaining α within the 60-75° range and using the baseline values for other parameters, the program is run using specified radial bandwidths of 1,2,5,10,25,100, and 200 km. Although the large bandwidths are not practical, they are used to determine the existence of any limiting conditions. These results, shown in Table IV (first entry is fuel burned in kg, second entry is actual radial band maintained in km), show that fuel required to maintain the orbit generally increases as the controlled radial bandwidth increases, with the exception being the 100 km band. Although the error between the radial band maintained and the pre-specified band is minimized as α increases, the maintained band cannot be correlated to the pre-specified band (changing any parameter changes the maintained band). For this reason, the radial bands discussed throughout this analysis are pre-

Table IV MASS OF FUEL BURNED (kg) AND ACTUAL RADIAL BAND MAINTAINED (km)

Band	$\alpha=60$	$\alpha=65$	$\alpha=70$	$\alpha=75$
1	1537/0.7	1684/0.7	2025/1.0	2627/1.2
2	2049/2	2013/1.8	2174/1.8	2683/2
5	2516/12	2628/8	2583/6	3065/5
10	2392/25	2554/16	3191/13	3602/11
25	2643/55	2828/43	3243/35	3595/30
50	2812/90	3049/75	3136/65	4289/58
100	3020/130	2859/125	2826/60	3787/75
200	2993/130	3549/140	4470/120	5743/135

specified bands. Figures 1-3 of Appendix E show the mass of fuel burned using bang-bang control and forced Keplerian control for 2, 25, and 100 km bands with $\alpha=70^\circ$. As can be seen, the fuel used increases in a generally linear manner as the number of orbits increases. For the 100 km band, the fuel used is linear when the points at the end of each burn are connected, as indicated by the dotted line in Figure 3. Thus, these results can be extrapolated for any number of orbits to give fuel usage vs Keplerian usage. However, the thrusters do not fire at the same point in each orbit (the thrusters fire approximately every three-fourths of an orbit for the cases of a small radial band and, thus firing precesses each orbit). These results are consistent throughout the analysis.

A constant radial band is maintained for α of approximately 65-70° but not for 60 and 75°, as shown in Figures 4-7 of Appendix E, which again verifies the required thrust angle. These figures are for a pre-specified radial bandwidth of 25 km, the results are similar for bandwidths of 1-50 km. Figure 8 of Appendix E shows the results for a pre-specified bandwidth of 100 km and an α of 70° (this is representative of results for $\alpha=60-75^\circ$ and bands of 100 km and greater). As can be seen, the band is wide enough that thrusters fire infrequently to reboost the satellite. The actual radial bandwidth maintained was then compared to the specified band. Based on these results, all subsequent analysis is performed for three cases of radial bandwidth; 2, 25, and 100 km. This will give results for a small, medium and large bandwidths, while examining the unusual results at 100 km.

C. VARIATION OF ATMOSPHERIC SCALE HEIGHT, β

Of the three variable parameters in the non-dimensionalized equations, β should have the most predictable effect on the results and is analyzed first. Using baseline values for other parameters, β is varied from $1.0e-10$ to $1.0e-2$, and results are examined for logical trends. Logic would dictate that increasing the value of β will increase the rate of orbital decay within the band, requiring more thruster firings to reboost the satellite,

and thus require more fuel. This is indeed the case as the results in Appendix F show. Figure 1 shows the fuel used as a function of β for a pre-specified 2 km band, while Figures 2 and 3 show the same results for 25 and 100 km bands, respectively. All three plots are similar in appearance indicating changes in β affect orbital decay uniformly over the range of bands. Below a certain value, $1e-5$ for 2 km band, changes in β have no effect on fuel usage. Above a certain value, $1e-3$ for 2 km band, the orbit decays too quickly for thrusters to control. In between these values, increases in β increasingly affect the fuel used. Since changes in β do not affect the forced Keplerian solution, the mass of fuel required for forced Keplerian maintenance for all cases is approximately 649 kg. Thus, smaller values of β allow the bang-bang control to be closer in efficiency to forced Keplerian motion. Analysis of the plots for radial band again show that a radial band is not maintained for 60 or 75° thrust angle, but is maintained and optimized in the 65-70° range. From these results, it is shown that changes in β affect the efficiency of bang-bang control as expected and are predictable.

D. VARIATION OF THRUST, T

The next variable to be analyzed is thrust (T). As explained in Chapter 3, either thrust or nondimensionalized thrust can be varied and the results will be the same.

Thrust is chosen because variations in thrust are more easily related to and understood. For this analysis, thrust is varied over the range 10-1000 N, while all other parameters are fixed at the baseline value. Figures 1-3 of Appendix G show the fuel required, for $\alpha=70^\circ$, to maintain 2, 25, and 100 km pre-specified bands, respectively.

Trends are similar on all three graphs. Fuel usage starts off low for small values of thrust, with thrust being small enough to produce quasi-forced Keplerian motion (thrusters fire for majority of time to reboost satellite). Forced Keplerian thrust is determined to be approximately 2.8 N for the reference conditions. To obtain this value of transverse thrust using a thrust angle of 70° would require a thrust of approximately 11.1 N. Thus, small values of thrust may produce a quasi-forced Keplerian motion with respect to the transverse thrust component. This is followed by a period of increased fuel usage as thrust increases. In the 2 km band case, increasing thrust further shows a drop in fuel usage followed by a relatively constant fuel usage as thrust increases above 300 N. The 25 km band case shows more fluctuation in fuel usage as thrust increases, followed again by a relatively constant fuel usage as thrust increases above 300 N. For the 100 km band case, increasing thruster size generally increases fuel

usage except for a fairly constant region in the range of 50-250 N.

Thus, other than a possible minimizing of fuel usage due to this apparent quasi-forced Keplerian motion, changes in thrust appear to have little effect on the optimality problem. The smaller fuel usage totals at low thrust (25-50 N) may be indicative of approaching a quasi-forced Keplerian motion (except thruster angle is 70° vice 0°). For all three cases, as thrust increases, fuel usage appears to approach a constant value. An optimal thrust angle of $65-70^\circ$ is again verified in this portion of the analysis.

E. VARIATIONS IN NONDIMENSIONALIZED BALLISTIC COEFFICIENT

The last parameter to be analyzed is nondimensional ballistic coefficient, \bar{B} . By nondimensionalizing, variations in B will encompass variations in the individual parameters of mass, atmospheric density, coefficient of drag, and reference surface area, as well as combinations of variations involving these parameters.

Analysis is conducted by varying \bar{B} over the range $4e3-2e5$ and comparing mass of fuel burned using bang-bang control (MFB) to mass of fuel burned using forced Keplerian motion (MFBK). This analysis is conducted for the three bands of 2, 25, and 100 km using baseline values for other parameters while varying α from $60-75^\circ$. Figures 1 and 2 of Appendix H show the results for the 2 km band case, results

for the 25 and 100 km bands are similar. As seen, the mass or fuel burned for both bang-bang control and forced Keplerian motion decreases as \bar{B} increases, approaching a constant value as \bar{B} increases above $2e5$. For optimality, maximizing \bar{B} minimizes fuel usage.

However, this does not give a feel for how efficient bang-bang control is compared to forced Keplerian motion. To analyze this, the ratio of MFB to MFBK is plotted versus \bar{B} for 2, 25, and 100 km bands and α of 65 and 70°. These results are shown in Figures 3-8 of Appendix H. Again, \bar{B} is varied over the range $4e3-2e5$. Values of \bar{B} below and above this range (and the range plotted for 100 km band) cause the orbit to decay too rapidly or too slowly, respectively. Logically, this is analogous to increasing the atmospheric density to a value that causes the orbit to decay faster than thrusters can maintain, or decreasing the atmospheric density to a value that causes the orbit to decay so slowly that the thrusters never fire in 100 orbits (thus giving no data since at least one firing of the thrusters in bang-bang control is required for comparison to forced Keplerian motion).

As seen in Figures 3-8, the general results for α of 65 and 70° are similar for all three bands. Also, the results for all three bands show a roughly constant value for the ratio of MFB to MFBK, with the 2 km band being most

efficient compared to forced Keplerian motion, followed by the 100 km band and then the 25 km band. A value of 1 for the ratio would indicate that the bang-bang control was equally efficient to Keplerian motion. Values less than 1 would indicate that the bang-bang control is superior to Keplerian motion and would numerically validate the theoretical results of Ross and Melton [Ref. 3]. The results shown are consistently above a ratio of 3, indicating that forced Keplerian motion is significantly more efficient than bang-bang control over all values of \bar{E} .

Throughout this analysis, the optimality of α in the range of 65-70° was verified. This result has remained valid throughout all of the analyses conducted, indicating that this is a globally valid result.

VI. CONCLUSIONS AND RECOMMENDATIONS

The purpose of this thesis was to determine if there are any cases where fixed angle, bang-bang control, orbital maintenance approaches or exceeds the efficiency of forced Keplerian motion as proposed by Ross and Melton [Ref. 3]. By nondimensionalizing the equations, a thorough study of the effects of all parameter combinations was possible. Analysis of the results indicate that, in all cases, forced Keplerian motion is superior to bang-bang control. There are no cases where bang-bang control even remotely approaches the efficiency of forced Keplerian motion. Thus, these results appear to be globally valid.

The optimality question for thrust angle also appears to be resolved globally. In all cases, the thrust angle is required to be between 65 and 70° in order to maintain a constant radial band. Generally, minimizing this angle improves fuel consumption, so the angle should be minimized as far as practicable while ensuring a constant radial band.

Maintenance of a pre-specified radial bandwidth is not always possible or predictable for this control strategy. The error between specified and maintained band can be minimized through proper bandwidth selection. Selecting a relatively small, 2 km, or large, 100 km, band minimizes

the error. Also, maximizing the thrust angle, α , generally minimizes the error, and thus, α should be set as high as possible, while maintaining a constant radial band. Since this contradicts the requirement to minimize α for fuel savings, trade-offs must be considered. Minimizing the specified bandwidth moves the efficiency of bang-bang control closer to that of forced Keplerian motion.

The effects of changes in atmospheric scale height, β , are logical and predictable on the effects of the mass of fuel burned in bang-bang control. Since, by definition, changes in β do not affect forced Keplerian results, the changes in mass burned in bang-bang control directly correlate to changes in efficiency. Thus, the lower the value of β , the more efficient bang-bang control is in relation to Keplerian motion.

The effects of varying thrust are not so predictable; however, general trends can be inferred from the results. Low values of thrust appear to approach quasi-forced Keplerian motion and are more efficient. Higher values of thrust increase the mass of fuel burned, however, a maximum limit appears to be approached. As in the case of β , changes in thrust do not affect the mass of fuel burned in Keplerian control, thus the mass of fuel burned in bang-bang control is indicative of the efficiency.

This is not the case for changes in \bar{B} , where changes affect the final Keplerian fuel usage. Thus, in order to

examine efficiency, the ratio of mass of fuel burned using bang-bang control to mass of fuel burned with Keplerian motion must be used. It was initially expected that changes in \bar{B} would have noticeable effects on efficiency and would show a trend that would indicate values where bang-bang control efficiency approached Keplerian efficiency. This is not the case, as changes in \bar{B} seem to have little effect on the ratio of efficiencies.

Thus, the superiority of forced Keplerian motion to fixed angle bang-bang control is globally confirmed. However, further research should be conducted into the solutions proposed by Ross and Melton [Ref.3]. Control using variable thrust angle bang-bang control (so-called Primer-vectoring) should be examined for comparison to these results. Also, fixed angle bang-bang control, as described here, should be compared with other innovative methods of control, as well as with the "Lambert control" used with the shuttle, for possible fuel savings for space-station type platforms.

The results of this thesis also suggest areas for further study. A method for maintaining a pre-specified band is highly desirable, but was not achieved in this study. Although the global validity of the thrust angle being required to be between 65 and 70° was shown, the reason for this has not been studied. The problem of

micro-gravity constraints and its effect on thruster firings and control strategies has also not been studied, but would be a critical factor in any control design. The fact that forced Keplerian motion has been shown to be on the order of three times more efficient than bang-bang control indicates that there is much room for research into further optimization techniques for bang-bang control. Finally, the question of practicality has not been addressed in relation to both forced Keplerian motion (generally not very practicable but very efficient) and bang-bang control (very practicable but not very efficient).

APPENDIX A

A. PROGRAM LISTING

```

C
C
C      OBJECTIVE: COMPARISON OF FORCED KEPLERIAN TO BANG-BANG
C                  CONTROL OF ORBITAL ALTITUDE
C
C
C      VARIABLE DEFINITIONS
C
C          XBAR(1)=NONDIMENSIONALIZED ORBITAL RADIUS
C          XBAR(2)=NONDIMENSIONALIZED ORBITAL RADIAL VELOCITY
C          XBAR(3)=THETA
C          XBAR(4)=NONDIMENSIONALIZED ORBITAL ANGULAR VELOCITY
C          XBDOT(1)=DERIVATIVE OF XBAR(1)
C          XBDOT(2)=DERIVATIVE OF XBAR(2)
C          XBDOT(3)=DERIVATIVE OF XBAR(3)
C          XBDOT(4)=DERIVATIVE OF XBAR(4)
C          RO=INITIAL ORBITAL RADIUS
C          R=ORBITAL RADIUS
C          RREF=REFERENCE ALTITUDE FOR DENSITY
C          D=DRAG (N)
C          DK=DRAG KEPLERIAN
C          E=SPECIFIC ENERGY
C          EO=SPECIFIC ENERGY AT INITIAL RADIUS RO
C          M=S/C MASS (KG)
C          MO=INITIAL S/C MASS (KG)
C          ME=ARBITRARY MASS FOR NONDIMENSIONALIZING (20000KG)
C          MBAR=NONDIMENSIONALIZED MASS
C          MF=MASS OF FUEL BURNED IN TIME INCREMENT
C          MFK=MASS OF FUEL BURNED PER TIME INCREMENT KEPLERIAN
C          MFT=MASS OF FUEL BURNED TOTAL
C          MFTK=MASS OF FUEL BURNED TOTAL WITH KEPLERIAN MOTION
C          GAMMAR=FLIGHT PATH ANGLE (RAD)
C          GAMMAD=FLIGHT PATH ANGLE (DEG)
C          TH=THRUST (N)
C          THK=KEPLERIAN THRUST
C          THMAX=BLOWDOWN (MAX) THRUST (N)
C          THBAR=NONDIMENSIONALIZED THRUST =(TH*TAU**2)/(MR)
C          THBM=NONDIMENSIONALIZED BLOWDOWN (MAX) THRUST
C          ALPHAR=THRUST ANGLE (RAD)
C          B=BALLISTIC COEFFICIENT (M/(CD*S))
C          BBAR=NONDIMENSIONALIZED B =B/(RHO0*RE)
C          RHO=CALCULATED ATMOSPHERIC DENSITY
C          RHO0=REFERENCE ATMOSPHERIC DENSITY
C          SPI=SPECIFIC IMPULSE
C          V=VELOCITY
C          VBAR=NONDIMENSIONALIZED VELOCITY
C          G=GRAVITATIONAL ACCELERATION
C          SMA=SEMI-MAJOR AXIS
C          ECC=ECCENTRICITY
C          T=TIME
C          TINC=INCREMENT OF TIME(STEP SIZE)

```

```

C      TF=END TIME
C      PTI=PRINT TIME INTERVAL
C
C
C
C
C      CONSTANTS
C
C      RE=RADIUS      EARTH
C      MU=EARTHS GRAVITAIONAL CONSTANT
C      TAU=ORBITAL PERIOD AT RE
C
C      START PROGRAM
C      PROGRAM ORBMAINT
C
C      VARIABLE DECLARATION
C      IMPLICIT REAL*8(A-H,M-Z)
C      DIMENSION XBAR(4),XBDOT(4)
C
C      CONSTANT DEFINITIONS
C      PI=DATAN(1.0D+00)*4.0D+00
C      MU=3.98601208133D+14
C      G=9.806D+0
C      RE=6.3782D+6
C      TAU=2.*PI*RE**1.5/MU**0.5
C      J=4
C      ME=20000.D+0
C
C      INITIALIZE FUEL USAGE TOTALS
C
C      MFT=0.0D+0
C      MFTK=0.0D+0
C
C
C      CCCCCCCCCCCCCCCCCCCCCCCCCCCCCCCCCCCCCCCCCCCCCCCCCCCCCCCCCC
C      MAIN PROGRAM
C
C      OPEN(10,FILE='inp',STATUS='OLD')
C      OPEN(20,FILE='outp',STATUS='NEW')
C      OPEN(30,FILE='orbp',STATUS='NEW')
C      OPEN(40,FILE='ratp',STATUS='NEW')
C
C      READ INPUTS AND INITIALIZE PARAMETERS
C
C      READ(10,1)RO,MO,THMAX,TB,TFB,TINCB,PTIB,BBAR,BETA,SPI
1     FORMAT(10(/,21X,D13.7))
C
C      M=MO
C      MBAR=M/ME
C      TAURO=2.*PI*RO**1.5/MU**0.5
C      TINC=TINCB*TAU
C      THBM=THMAX*TAU*TAU/(ME*RE)
C
C      READ PARAMETERS THRUST ANGLE, DESIRED BAND,THRUST FACTOR
C
C      PRINT*, 'ENTER ALPHA'

```

```

C
C
C      READ*,ALPHA
C      ALPHAR=ALPHA*PI/180.0D+0
C
C
C      PRINT*, 'ENTER BAND, (KM)'
C      READ*,BAND
C      BAND=BAND*1000.0D+0
C
C
C      PRINT*, 'ENTER THFAC'
C      READ*,THFAC
C      THFAC=THFAC*1.0D+0
C
C      INITIALIZE COUNTERS USED IN PROGRAM
C
C      INDEX=0
C      KOUNT=1
C      TRAD=0.0D+0
C
C
C      INITIALIZE NONDIMENSIONALIZED STATE VARIABLES
C
C      XBAR(1)=R0/RE
C      XBAR(2)=0D+0
C      XBAR(3)=0D+0
C      XBAR(4)=2.0D+0*PI*TAU/TAURO
C
C      COMPUTE INITIAL ORBITS VELOCITY AND ENERGY
C
C      VO=(MU/R0)**0.5
C      EO=((VO*VO)/2.-MU/R0)
C
C      COMPUTE RADIUS,VELOCITY,ENERGY FOR DESIRED BAND MIN AND MAX
C
C      RMIN=R0-BAND/2.0
C      VMIN=(MU/RMIN)**0.5
C      EMIN=((VMIN*VMIN)/2.-MU/RMIN)
C
C      RMAX=R0+BAND/2.0
C      VMAX=(MU/RMAX)**0.5
C      EMAX=((VMAX*VMAX)/2.0-MU/RMAX)
C
C      SET UP OUTPUT FILE HEADERS
C
C      IBAND=INT(BAND)
C      ITHMAX=INT(THMAX)
C      IALPHA=INT(ALPHA)
C
C      WRITE(20,*) '!!BAND=',IBAND, ' THMAX=',ITHMAX, ' ALPHA=',IALPHA
C      WRITE(20,*) '!!EMIN=',EMIN, ' EMAX=',EMAX
C      WRITE(30,*) '!!BAND=',IBAND, ' THMAX=',ITHMAX, ' ALPHA=',IALPHA
C      WRITE(40,*) '!!BAND=',IBAND, ' THMAX=',ITHMAX, ' ALPHA=',IALPHA
C
C
C      WRITE(20,*) '!! ORBITS RADIUS VELOCITY MFB MFBK
C      * ANGM ENERGY'
C      WRITE(20,*) '!! (KM) (KM/SEC) (KG) (KG)'
C      WRITE(30,*) '!! ORBITS SMA ECC APOGEE PERIGEE
C      * PERIOD'
C      WRITE(40,*) '!! TIME ORBITS DRAG THRUST MASS
C      * GAMMA'

```



```

C      CALL SUBROUTINE ORBPAR TO COMPUTE ORBITAL PARAMETERS
C
C      CALL ORBPAR(ENERGY,ANGM,R,MU,PI,ECC,SMA,APOGEE,PERIGE,PERIOD)
C
C      COMPUTE NEW MBAR AND PUT R,V IN OUTPUT FORM
C
C      MBAR=M/ME
C      R=R/1000.0
C      V=V/1000.0
C
C      DATA OUT
C
C      CHECK TO SEE IF TIME TO PRINT OUTPUT
C
C      IF(KOUNT .LT. DNINT(PTIB/TINCB)) GO TO 200
C
C      PRINT OUTPUTS TO OUTPUT FILES OUT, RAT, ORB
C
C      WRITE(20,2)TB,R,V,MFT,MFTK,ANGM,E
C      FORMAT(2X,F6.2,2X,F9.3,2X,F7.4,2X,F8.2,2X,F8.2,2X,F12.0,
C      *2X,F10.0)
C
C      WRITE(30,3)TB,SMA,ECC,APOGEE,PERIGE,PERIOD
C      FORMAT(2X,F7.2,1X,F10.3,3X,F4.3,3X,F10.3,1X,F10.3,2X,F8.4)
C
C      WRITE(40,4)T,TB,D,TH,M,GAMMAD
C      FORMAT(2X,F8.0,1X,F6.2,2X,F12.9,3X,F5.0,5X,F9.3,1X,F10.4)
C
C      RESET COUNTER
C
C      KOUNT=0
C
C      CHECK TO SEE IF ORBIT COMPLETE, RESET ORBITAL ANGLE
C
C      IF (TRAD .GE. 1.0D+0) TRAD=0.0D+0
C
C      UPDATE COUNTER
C      200 KOUNT=KOUNT+1
C
C      CHECK FOR END OF PROGRAM
C
C      IF(TB .LT. TFB) GO TO 100
C
C      END
C
C      CCCCCCCCCCCCCCCCCCCCCCCCCCCCCCCCCCCCCCCCCCCCCCCCCCCCCCCCCCCCCC
C
C      THIS SUBROUTINE CALCULATES DRAG FOR USE IN THE EQUATIONS
C      OF MOTION.
C
C      SUBROUTINE DRAG(BBAR,RE,XBAR,BETA,MBAR,VBAR,D)
C      IMPLICIT REAL*8(A-H,M-Z)
C
C      DIMENSION XBAR(4)
C
C      SET REFERENCE ALTITUDE FOR ATMOSPHERIC DENSITY CALCULATIONS
C
C      RREF=6.638145D+6
C

```

```

C      COMPUTE PRESENT NONDIMENSIONALIZED VELOCITY
C      VBAR=((XBAR(2)*XBAR(2))+(XBAR(1)*XBAR(4))**2)**0.5
C
C      COMPUTE EXPONENTIAL TERM IN DRAG EQN
C
C      Z=EXP(-BETA*RE*(XBAR(1)-(RREF/RE)))
C
C      COMPUTE DRAG TERM
C
C      D=E*VBAR*VBAR/(2.0*MBAR*BBAR)
C
C
C      RETURN
C      END
C
C
C      CCCCCCCCCCCCCCCCCCCCCCCCCCCCCCCCCCCCCCCCCCCCCCCCCCCCCCCCCCCCCC
C
C      THIS SUBROUTINE UPDATES THE EQUATIONS
C      OF MOTION
C
C      SUBROUTINE EQN(D,XBAR,XBDOT,VBAR,THBAR,ALPHAR,MBAR,PI)
C      IMPLICIT REAL*8(A-H,M-Z)
C
C      DIMENSION XBAR(4),XBDOT(4)
C
C      A=XBAR(1)*XBAR(4)*XBAR(4)
C      B=4.0*PI*PI/(XBAR(1)*XBAR(1))
C      C=D*(XBAR(2)/VBAR)
C      E=THBAR*SIN(ALPHAR)/MBAR
C
C      F=2.0*XBAR(4)*XBAR(2)/XBAR(1)
C      G=(D/XBAR(1))*(XBAR(1)*XBAR(4)/VBAR)
C      H=THBAR*COS(ALPHAR)/(MBAR*XBAR(1))
C
C      XBDOT(1)=XBAR(2)
C      XBDOT(2)=A-B-C+E
C      XBDOT(3)=XBAR(4)
C      XBDOT(4)=-F-G+H
C
C
C      RETURN
C      END
C
C
C      CCCCCCCCCCCCCCCCCCCCCCCCCCCCCCCCCCCCCCCCCCCCCCCCCCCCCCCCCCCCCC
C
C      THIS SUBROUTINE CALCULATES ORBITAL PARAMETERS
C
C      SUBROUTINE ORBPAR(ENERGY,ANGM,R,MU,PI,ECC,SMA,APOGEE,PERIGE,
C      *PERIOD)
C      IMPLICIT REAL*8(A-H,M-Z)
C
C      PROBLEM COULD ARISE IN COMPUTING ECCENTRICITY IF VERY
C      SMALL- COULD TRY TO TAKE SQRT OF NEG NUMBER. TO
C      PREVENT, IF ECCENTRICITY IS LESS THAN 1E-6, SET
C      EQUAL TO 0.
C

```

```

PROB=(1.+2.*ENERGY*ANGM*ANGM/(MU*MU))
IF (DABS(PROB) .LT. 1.D-12) THEN
    ECC=0.0D+0
ELSE
    ECC=PROB**0.5
ENDIF

SMA=(-MU/(2.*ENERGY))/1000.0

SMAM=SMA*1000.0
APOGEE=SMA*(1.0+ECC)
PERIGE=SMA*(1.0-ECC)
PERIOD=2.0*PI*(SMAM**1.5)/(MU**0.5)/60.0

RETURN
END

CCCCCCCCCCCCCCCCCCCCCCCCCCCCCCCCCCCCCCCCCCCCCCCCCCCCCCCCCCCC
C      THIS SUBROUTINE DOES A FOURTH LEVEL RUNGE-KUTTA
C      INTEGRATION.
C
SUBROUTINE RK4(TB,XBAR,XBDOT,J,TINCB,INDEX)
IMPLICIT REAL*8(A-H,M-Z)
INTEGER INDEX,I

C
C      DIMENSION XBAR(4),XBDOT(4),SAVED(4),SAVEX(4)
C
C      INDEX=INDEX+1
C      GO TO (1,2,3,4),INDEX
C
1      DO 10 I=1,J
        SAVEX(I)=XBAP(I)
        SAVED(I)=XBDOT(I)
10     XBAR(I)=SAVEX(I)+0.5D+0*TINCB*XBDOT(I)
        TB=TB+0.5D+0*TINCB
        RETURN
C
C
2      DO 20 I=1,J
        SAVED(I)=SAVED(I)+2.D+0*XBDOT(I)
20     XBAR(I)=SAVEX(I)+0.5D+0*TINCB*XBDOT(I)
        RETURN
C
C
3      DO 30 I=1,J
        SAVED(I)=SAVED(I)+2.D+0*XBDOT(I)
30     XBAR(I)=SAVEX(I)+TINCB*XBDOT(I)
        TB=TB+0.5D+0*TINCB
        RETURN
C
C
4      DO 40 I=1,J
        XBAR(I)=SAVEX(I)+TINCB/6.D+0*(SAVED(I)+XBDOT(I))
40     INDEX=0
        RETURN
C
C

```

```

      END
C
CCCCCCCCCCCCCCCCCCCCCCCCCCCCCCCCCCCCCCCCCCCCCCCCCCCCCCCCCCCC
C
C      THIS SUBROUTINE DETERMINES IF THRUSTERS SHOULD BE ON OR
C      OFF TO TRY TO STAY WITHIN THE DESIRED BAND
C
C      SUBROUTINE THRUST(E0,XBAR,THBAR,THFAC,RMIN,EMAX,E,ETH,
C      *THBM)
C      IMPLICIT REAL*8(A-H,M-Z)
C
C      DIMENSION XBAR(4),XBDOT(4)
C
C      RE=6.3782D+6
C
C      COMPUTE NONDIMENSIONALIZED POINT FOR THRUSTERS TO TURN ON
C      BASED ON RADIUS.
C
C      RTH=RMIN/RE
C
C      ETH=EMAX-(EMAX-EMIN)*THFAC
C
C      IF THRUSTERS ARE ON GO TO SEE IF TIME TO TURN OFF
C
C      IF (THBAR .EQ. THBM) GO TO 100
C
C      CHECK IF RADIUS BELOW BAND
C
C      IF (XBAR(1) .LE. RTH) THEN
C
C          CHECK IF ENERGY BELOW INITIAL ENERGY
C
C          IF (E .LE. E0) THEN
C
C              TURN THRUSTERS ON
C
C              THBAR=THBM
C
C          ELSE
C
C              OTHERWISE LEAVE OFF
C
C              THBAR=0D+0
C          ENDIF
C
C      RADIUS NOT BELOW BAND, LEAVE OFF THRUSTERS
C
C      ELSE
C
C          THBAR=0D+0
C      ENDIF
C
C      IF THRUSTERS ARE ON, SEE IF TIME TO TURN OFF
C
C      100 IF (E .GE. E0) THBAR=0D+0
C
C      RETURN
C      END
C
CCCCCCCCCCCCCCCCCCCCCCCCCCCCCCCCCCCCCCCCCCCCCCCCCCCCCCCCCCCC

```

B. SAMPLE INPUT FILE

```

5.6381450D+06
2.0000000D+04
3.0000000D+02
0.0000000D+00
1.0000000D+02
2.0000000D-04
1.0000000D-01
2.5000000D+04
2.1200000D-05
3.0000000D+02

```

C. SAMPLE OUTPUT FILE

```

BAND= 25000 THMAX= 300 ALPHA= 70
EMIN= -30080181.48670808 EMAX= -29967109.06483507
ORBITS RADIUS VELOCITY MFB MFBK ANG M ENERGY
      (KM) (KM/SEC) (KG) (KG)
1.00 6636.385 7.7501 0.00 6.49 51432570538. -30031067.
2.00 6634.580 7.7512 0.00 12.98 51425887643. -30038873.
3.00 6632.737 7.7523 0.00 19.47 51418951743. -30046977.
4.00 6630.855 7.7534 0.00 25.96 51411742642. -30055404.
5.00 6628.930 7.7545 0.00 32.45 51404237633. -30064181.
6.00 6626.951 7.7557 0.00 38.94 51396411113. -30073338.
7.00 6634.414 7.7513 110.11 45.43 51425131788. -30039612.
8.00 6628.660 7.7600 187.56 51.91 51438552722. -30023833.
9.00 6625.232 7.7641 224.78 58.40 51438811678. -30023532.
10.00 6622.517 7.7673 259.52 64.89 51438814899. -30023533.
11.00 6620.638 7.7695 293.54 71.38 51438812800. -30023539.
12.00 6619.667 7.7706 327.04 77.87 51438816720. -30023537.
13.00 6619.631 7.7706 359.91 84.36 51438831447. -30023522.
14.00 6620.517 7.7696 392.48 90.85 51438826115. -30023529.
15.00 6622.261 7.7676 425.88 97.34 51438818018. -30023539.
16.00 6624.814 7.7642 452.25 103.83 51435956478. -30026876.
17.00 6628.234 7.7599 483.47 110.32 51434560951. -30028501.
18.00 6632.050 7.7555 519.87 116.81 51434837100. -30028179.
19.00 6636.064 7.7509 556.16 123.30 51435080714. -30027896.
20.00 6640.091 7.7462 592.24 129.79 51435311164. -30027628.
21.00 6643.950 7.7417 628.33 136.28 51435512393. -30027394.
22.00 6647.468 7.7377 663.58 142.76 51435699197. -30027178.
23.00 6650.501 7.7342 699.25 149.25 51435880508. -30026968.
24.00 6652.923 7.7314 734.93 155.74 51436047241. -30026776.

```

25.00	6654.639	7.7294	770.60	162.23	51436208297.	-30026590.
26.00	6655.596	7.7283	806.27	168.72	51436378759.	-30026392.
27.00	6655.751	7.7281	841.63	175.21	51436530808.	-30026217.
28.00	6655.108	7.7289	876.99	181.70	51436685225.	-30026038.
29.00	6653.711	7.7306	911.83	188.19	51436850956.	-30025846.
30.00	6651.615	7.7330	947.19	194.68	51437006143.	-30025666.
31.00	6648.943	7.7362	981.93	201.17	51437196213.	-30025446.
32.00	6645.784	7.7399	1016.57	207.66	51437368920.	-30025245.
33.00	6642.315	7.7440	1051.21	214.15	51437587533.	-30024991.
34.00	6638.654	7.7483	1085.74	220.64	51437799569.	-30024744.
35.00	6634.978	7.7526	1120.38	227.13	51438037086.	-30024467.
36.00	6631.441	7.7568	1154.81	233.62	51438289123.	-30024173.
37.00	6628.199	7.7606	1189.65	240.10	51438574149.	-30023840.
38.00	6625.379	7.7639	1223.36	246.59	51438836529.	-30023533.
39.00	6623.118	7.7666	1255.62	253.08	51438840830.	-30023530.
40.00	6621.515	7.7684	1286.84	259.57	51438834154.	-30023540.
41.00	6620.631	7.7695	1317.86	266.06	51438836523.	-30023538.
42.00	6620.505	7.7696	1348.26	272.55	51438836153.	-30023539.
43.00	6621.127	7.7689	1379.38	279.04	51438840521.	-30023533.
44.00	6622.477	7.7673	1410.30	285.53	51438837255.	-30023536.
45.00	6624.516	7.7646	1436.45	292.02	51436551488.	-30026202.
46.00	6627.376	7.7609	1462.20	298.51	51434160812.	-30028987.
47.00	6630.657	7.7571	1496.42	305.00	51434443176.	-30028656.
48.00	6634.186	7.7530	1529.72	311.49	51434694318.	-30028363.
49.00	6637.818	7.7488	1563.32	317.98	51434926906.	-30028091.
50.00	6641.411	7.7446	1597.65	324.47	51435148627.	-30027833.
51.00	6644.824	7.7407	1631.46	330.95	51435348781.	-30027600.
52.00	6647.925	7.7371	1664.65	337.44	51435535867.	-30027382.
53.00	6650.596	7.7340	1698.46	343.93	51435712082.	-30027177.
54.00	6652.744	7.7315	1732.27	350.42	51435892956.	-30026967.
55.00	6654.278	7.7298	1765.66	356.91	51436042361.	-30026794.
56.00	6655.151	7.7288	1799.68	363.40	51436201010.	-30026610.
57.00	6655.343	7.7286	1833.38	369.89	51436371724.	-30026411.
58.00	6654.841	7.7292	1867.40	376.38	51436530981.	-30026227.
59.00	6653.669	7.7306	1901.31	382.87	51436693930.	-30026037.
60.00	6651.866	7.7327	1934.71	389.36	51436843665.	-30025863.
61.00	6649.535	7.7354	1969.04	395.85	51437033997.	-30025642.
62.00	6646.736	7.7387	2003.05	402.34	51437203180.	-30025445.
63.00	6643.614	7.7424	2036.66	408.83	51437417724.	-30025195.
64.00	6640.256	7.7464	2070.47	415.32	51437615550.	-30024965.
65.00	6636.822	7.7504	2103.76	421.80	51437843332.	-30024699.
66.00	6633.438	7.7544	2136.74	428.29	51438096137.	-30024404.
67.00	6630.226	7.7582	2170.24	434.78	51438361782.	-30024093.

68.00	6627.315	7.7616	2203.95	441.27	51438659553.	-30023745.
69.00	6624.808	7.7646	2236.21	447.76	51438839896.	-30023534.
70.00	6622.832	7.7669	2267.43	454.25	51438841147.	-30023534.
71.00	6621.455	7.7685	2298.14	460.74	51438854059.	-30023529.
72.00	6620.730	7.7694	2328.33	467.23	51438848302.	-30023528.
73.00	6620.676	7.7694	2358.32	473.72	51438838835.	-30023539.
74.00	6621.291	7.7687	2389.23	480.21	51438840540.	-30023537.
75.00	6622.551	7.7672	2419.84	486.70	51438841940.	-30023534.
76.00	6624.435	7.7647	2446.10	493.19	51436666305.	-30026071.
77.00	6627.090	7.7612	2471.84	499.68	51433850507.	-30029352.
78.00	6630.147	7.7576	2505.45	506.17	51434145633.	-30029006.
79.00	6633.448	7.7538	2538.84	512.66	51434396247.	-30028713.
80.00	6636.870	7.7499	2572.24	519.14	51434642574.	-30028425.
81.00	6640.288	7.7459	2605.53	525.63	51434851838.	-30028181.
82.00	6643.582	7.7421	2639.14	532.12	51435066093.	-30027931.
83.00	6646.639	7.7386	2672.94	538.61	51435260419.	-30027705.
84.00	6649.350	7.7354	2706.03	545.10	51435436862.	-30027500.
85.00	6651.626	7.7328	2739.84	551.59	51435610960.	-30027297.
86.00	6653.393	7.7308	2773.55	558.08	51435778411.	-30027103.
87.00	6654.598	7.7294	2806.74	564.57	51435948364.	-30026905.
88.00	6655.195	7.7287	2840.13	571.06	51436102292.	-30026727.
89.00	6655.170	7.7288	2874.05	577.55	51436255865.	-30026549.
90.00	6654.533	7.7295	2907.24	584.04	51436418385.	-30026360.
91.00	6653.305	7.7310	2940.53	590.53	51436578220.	-30026174.
92.00	6651.546	7.7331	2974.03	597.02	51436757933.	-30025965.
93.00	6649.293	7.7357	3007.74	603.51	51436918736.	-30025778.
94.00	6646.656	7.7388	3041.55	609.99	51437110521.	-30025555.
95.00	6643.718	7.7423	3075.35	616.48	51437314954.	-30025317.
96.00	6640.575	7.7460	3109.16	622.97	51437527062.	-30025070.
97.00	6637.340	7.7498	3142.25	629.46	51437748538.	-30024811.
98.00	6634.132	7.7536	3175.44	635.95	51437987351.	-30024532.
99.00	6631.065	7.7572	3208.84	642.44	51438257984.	-30024216.
100.00	6628.231	7.7605	3242.54	648.93	51438533304.	-30023894.

APPENDIX B

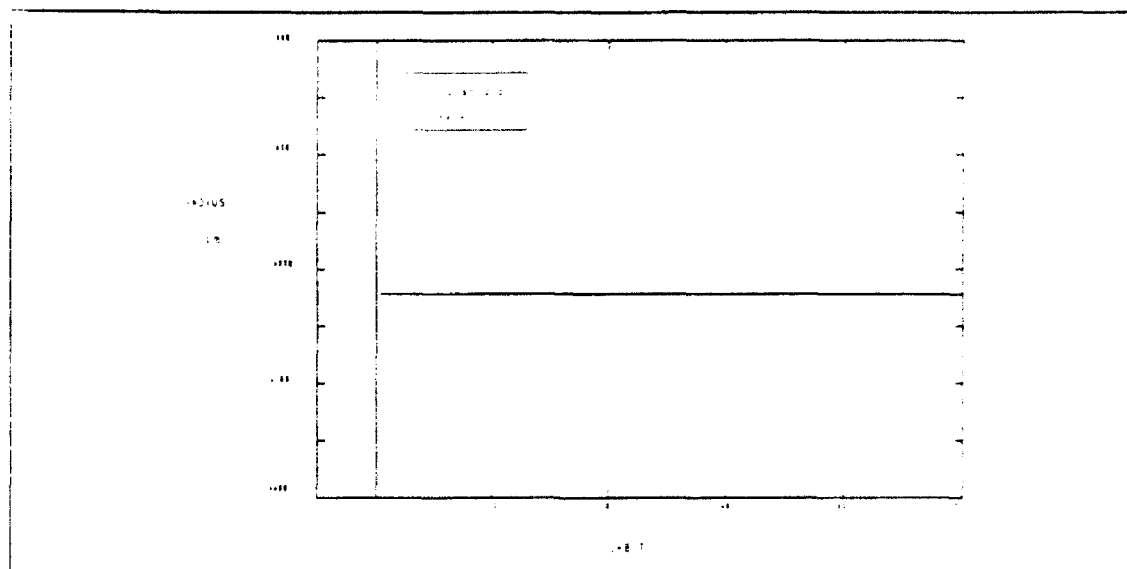


Figure 1

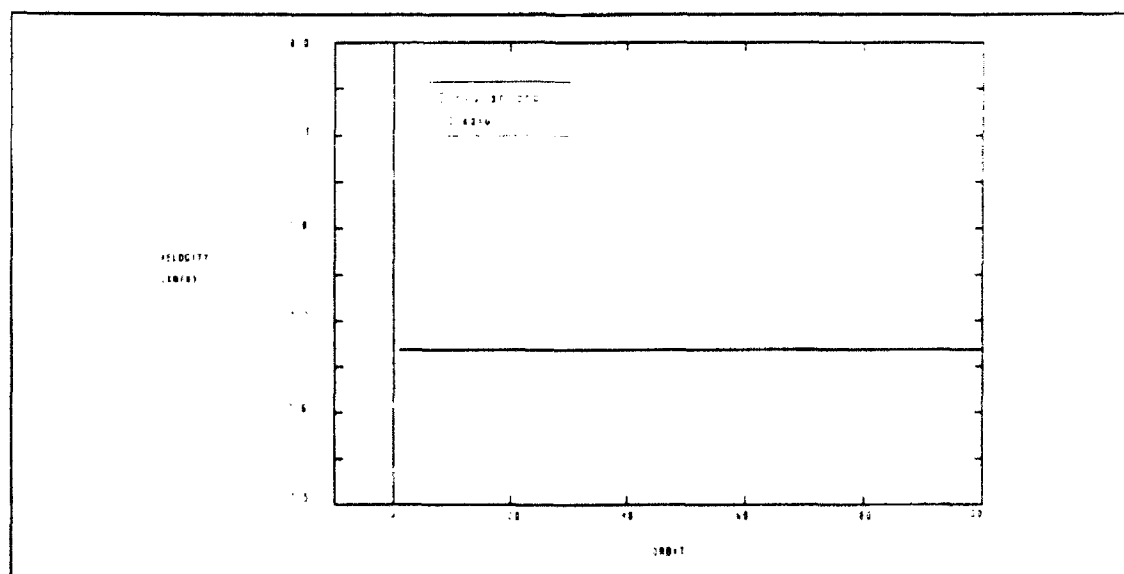


Figure 2

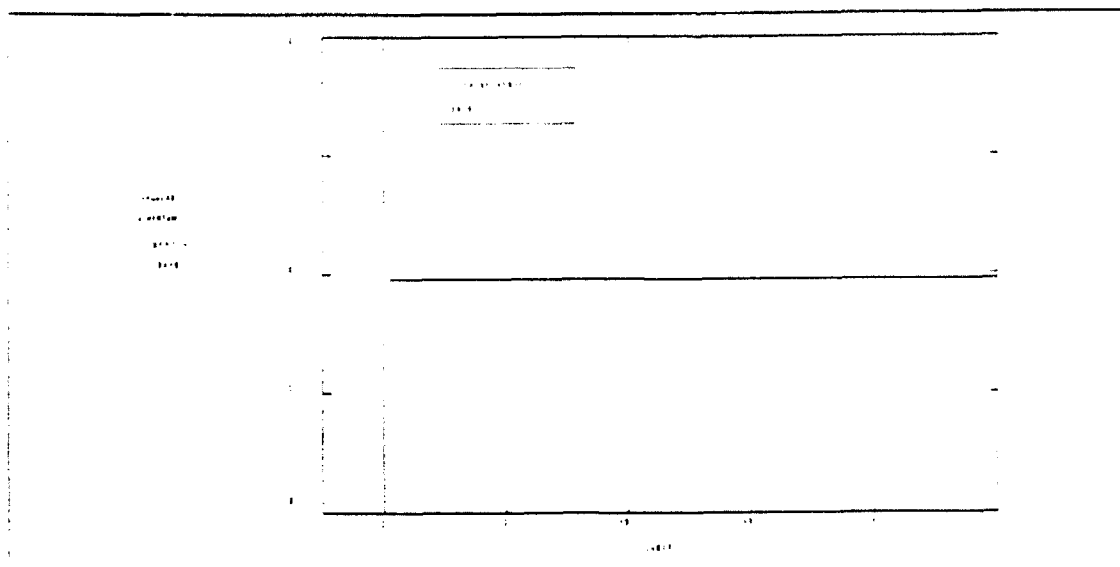


Figure 3

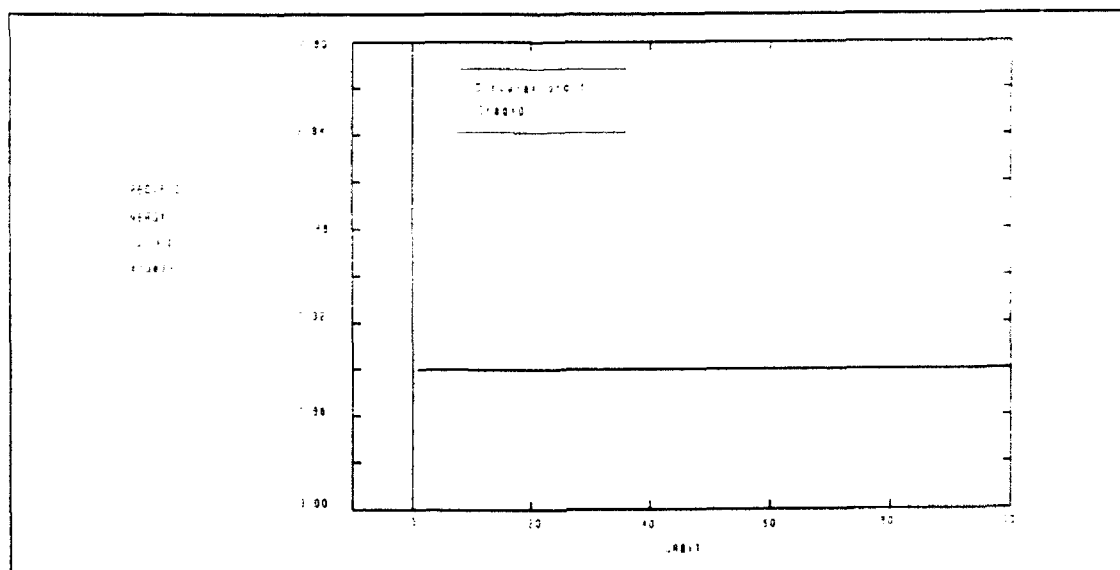


Figure 4

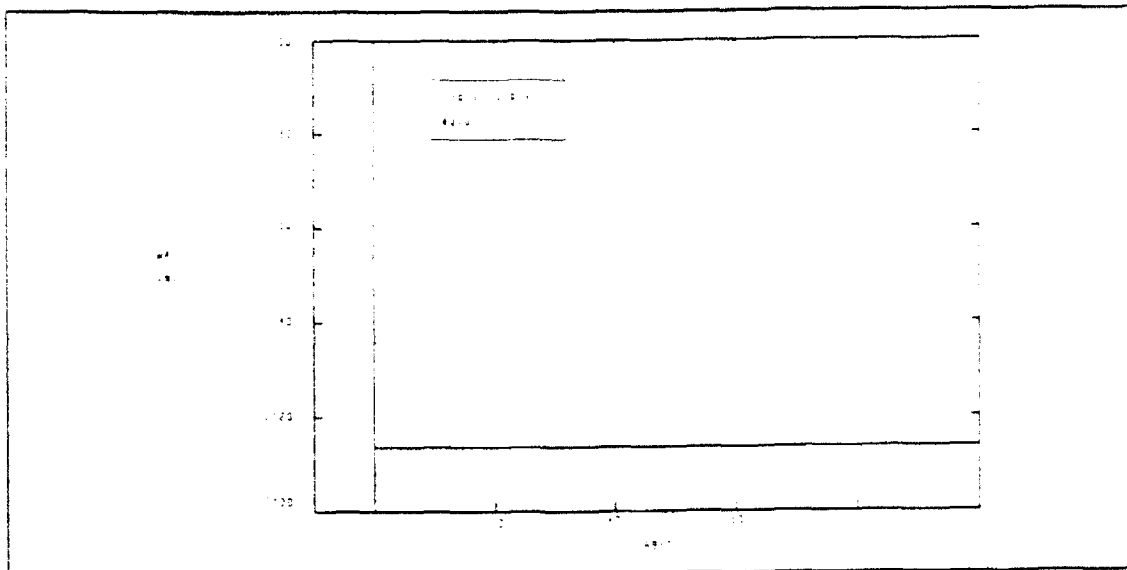


Figure 5

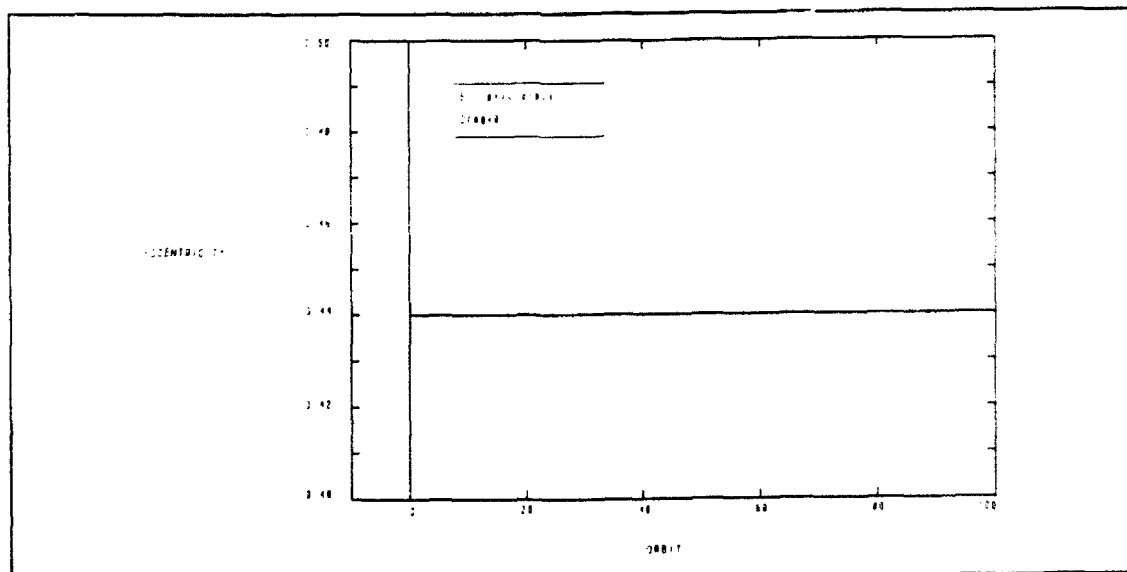


Figure 6

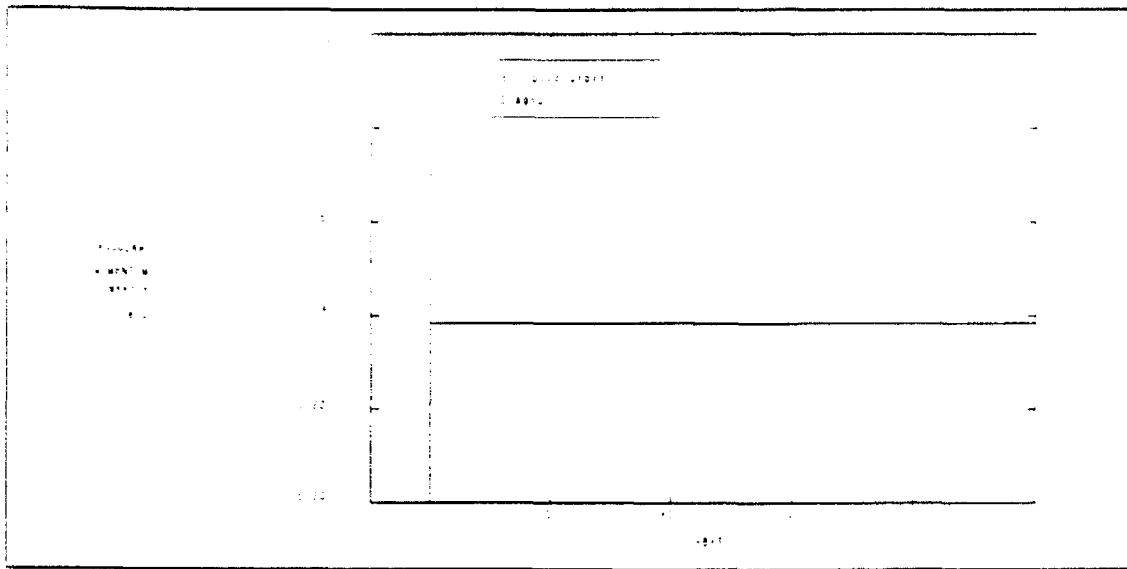


Figure 7

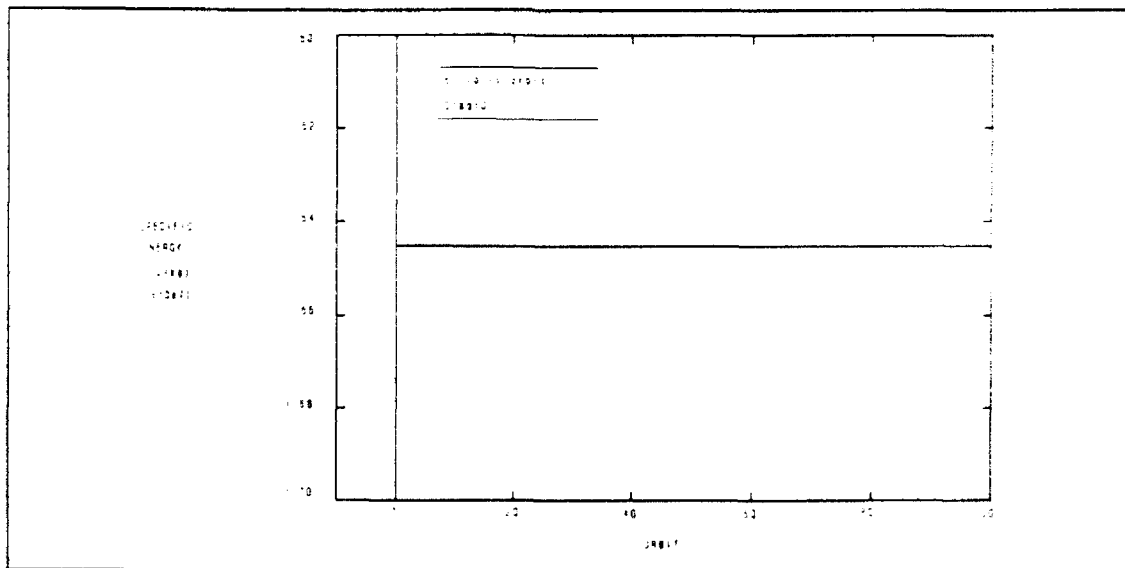


Figure 8

APPENDIX C

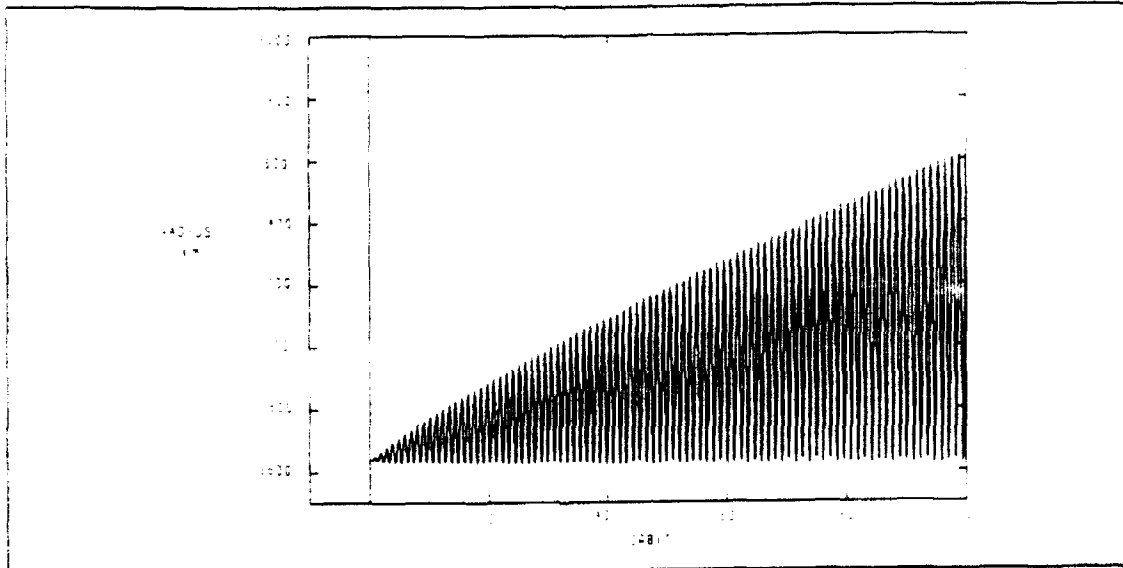


Figure 1

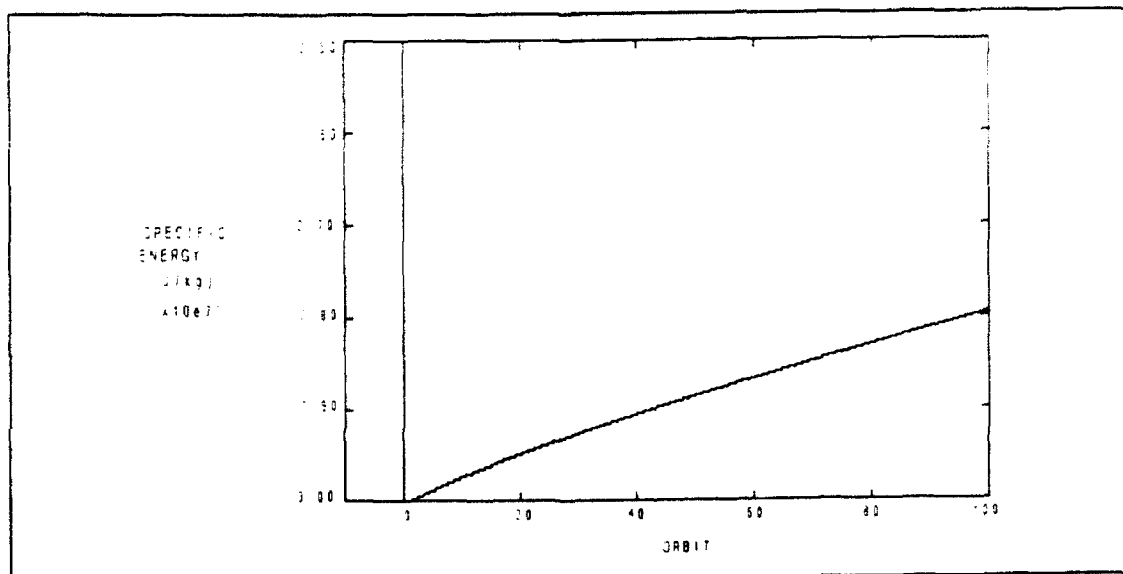


Figure 2

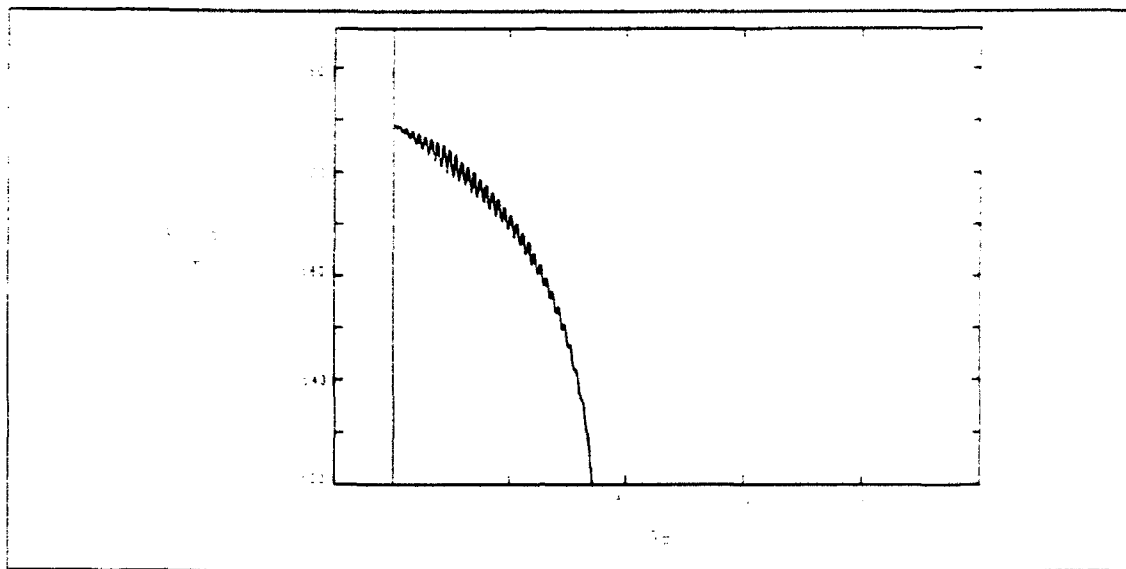


Figure 3

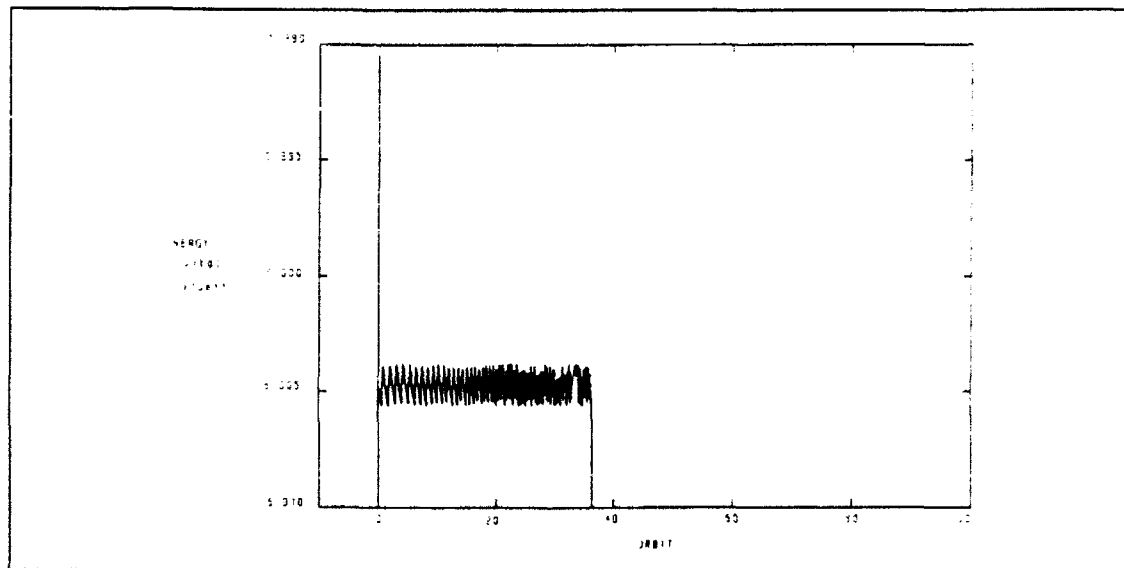


Figure 4

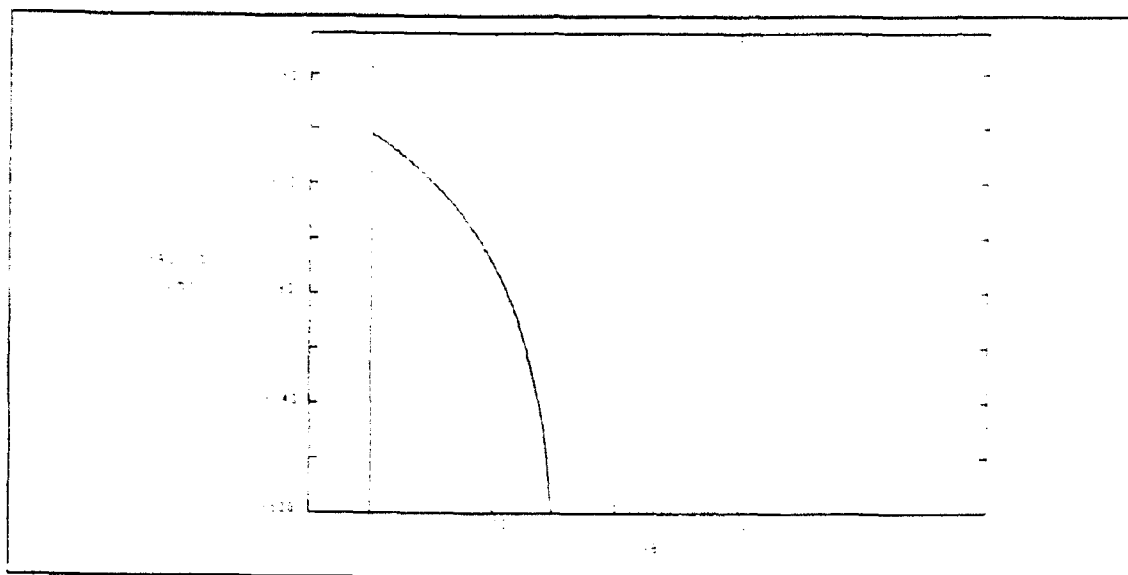


Figure 5

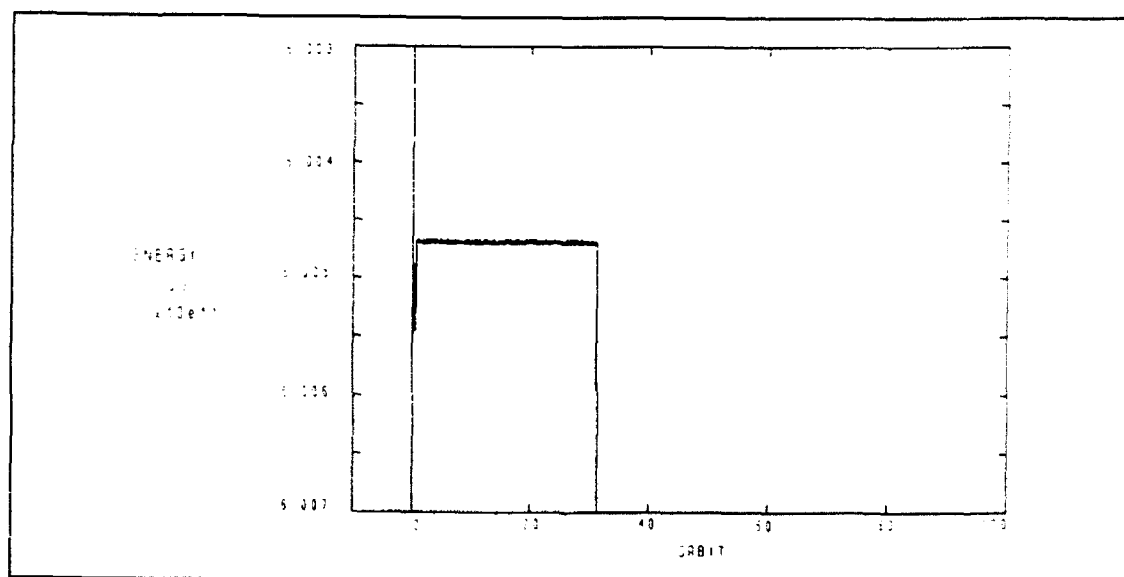


Figure 6

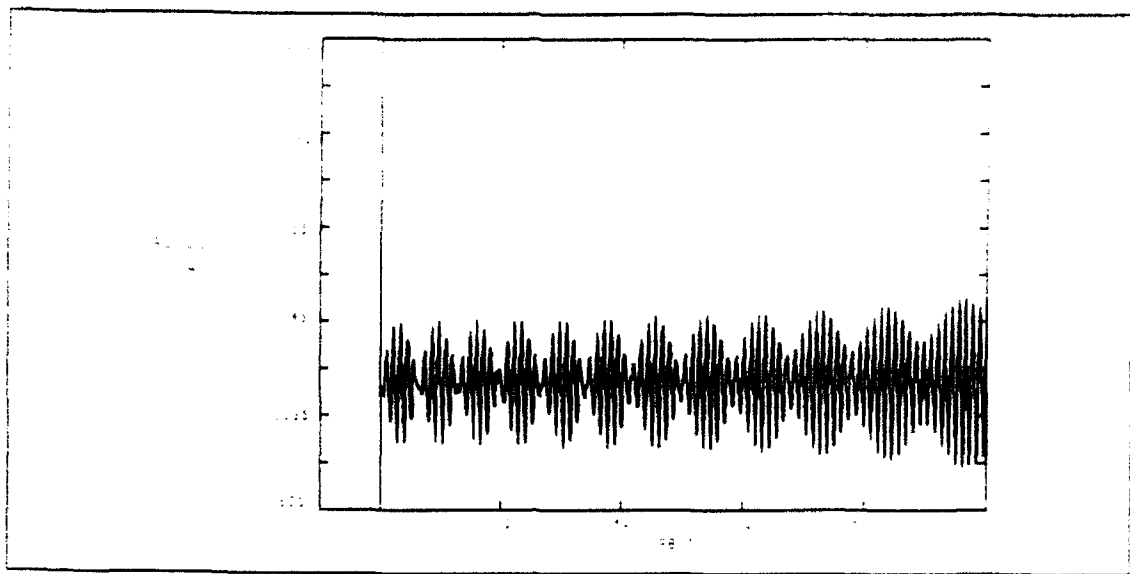


Figure 7

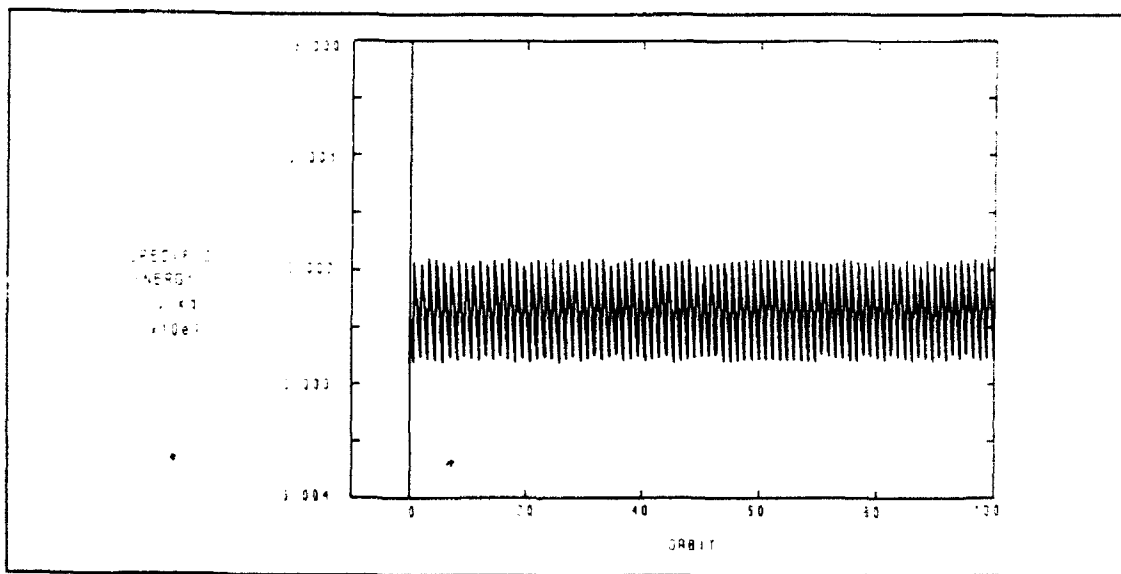


Figure 8

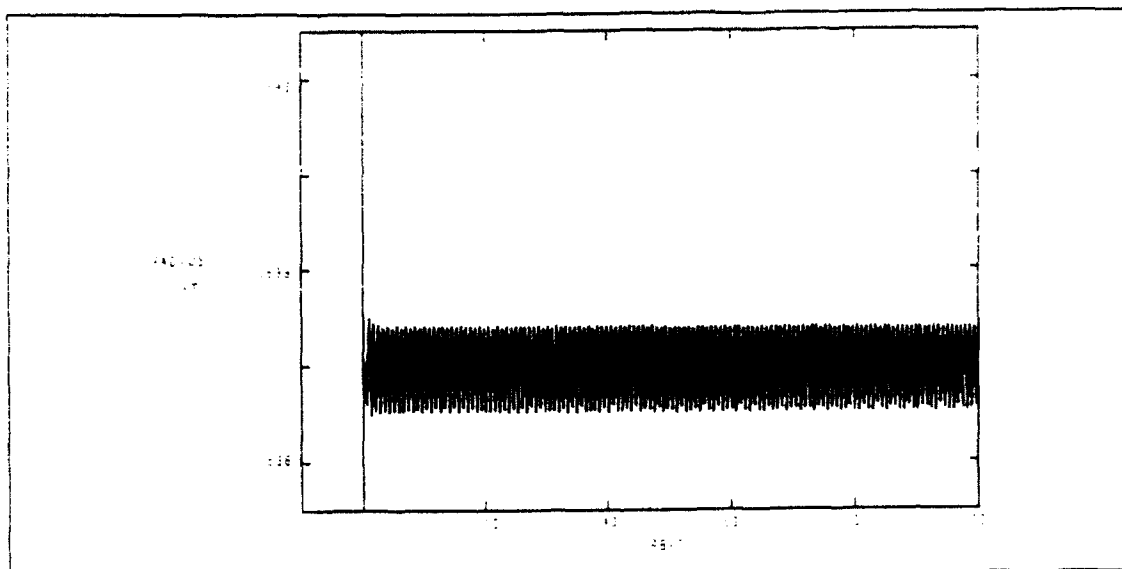


Figure 9

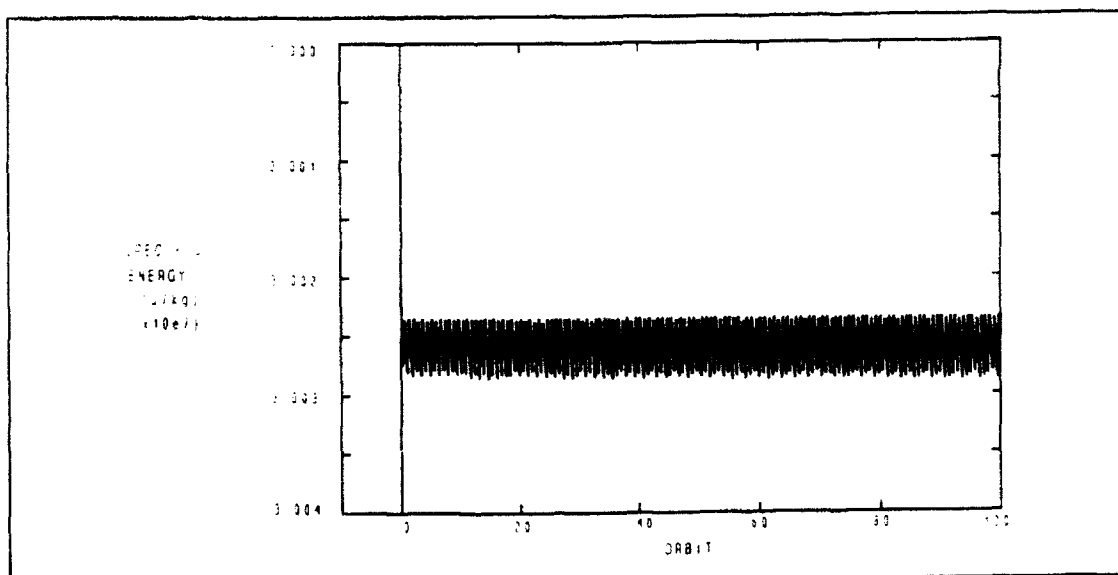


Figure 10

APPENDIX D

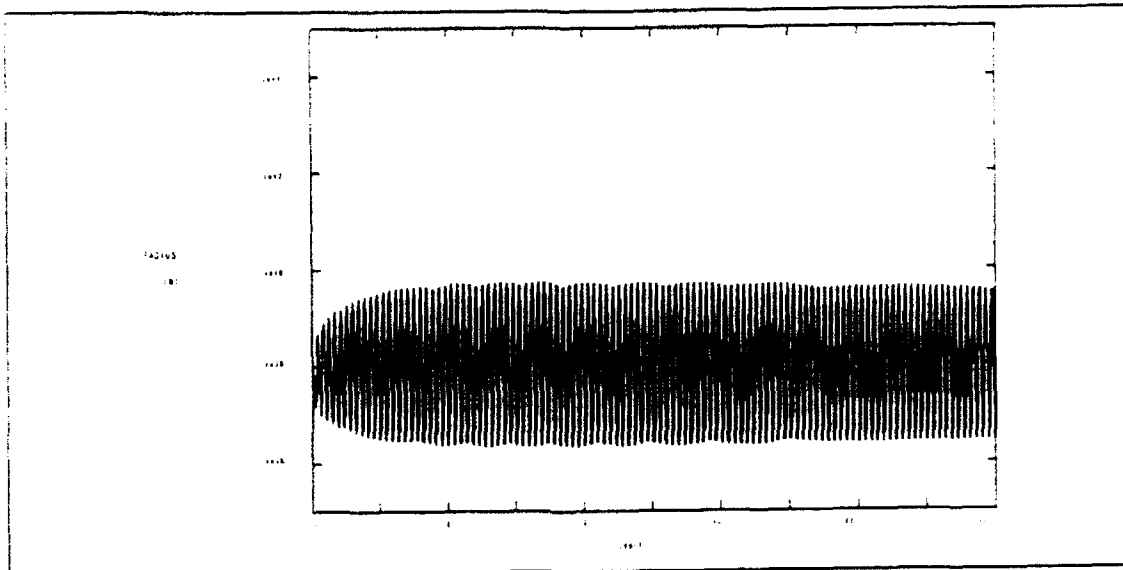


Figure 1 $\alpha = 60^\circ$

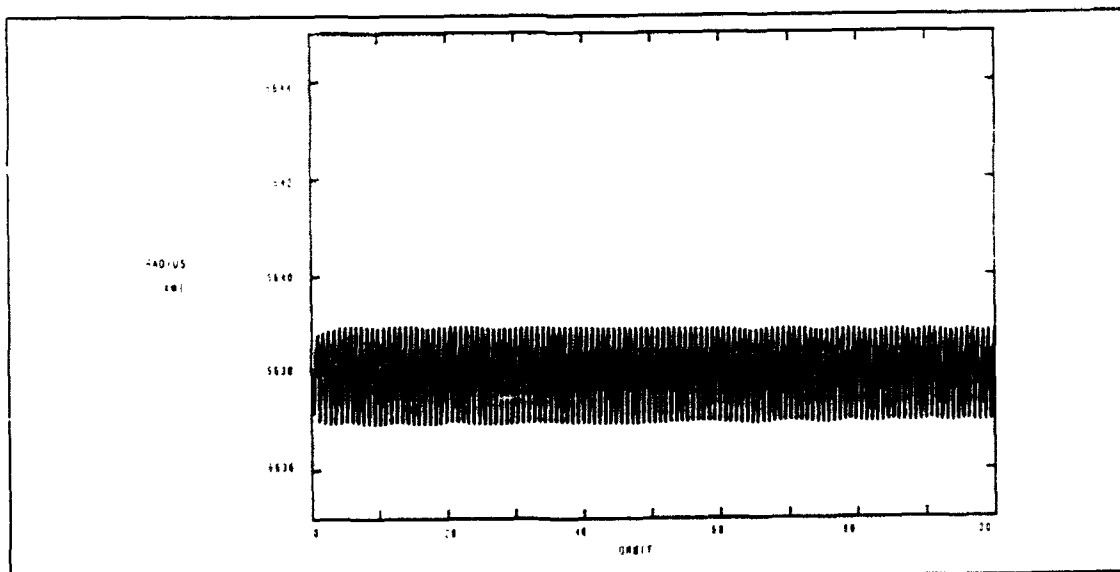


Figure 2 $\alpha = 65^\circ$

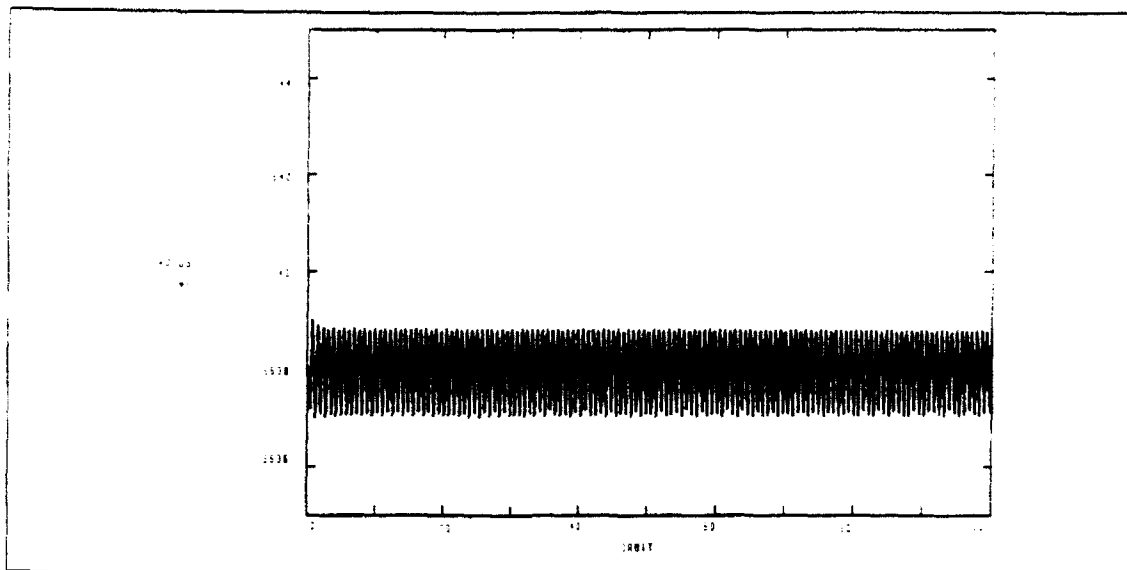


Figure 3 $\alpha=70^\circ$

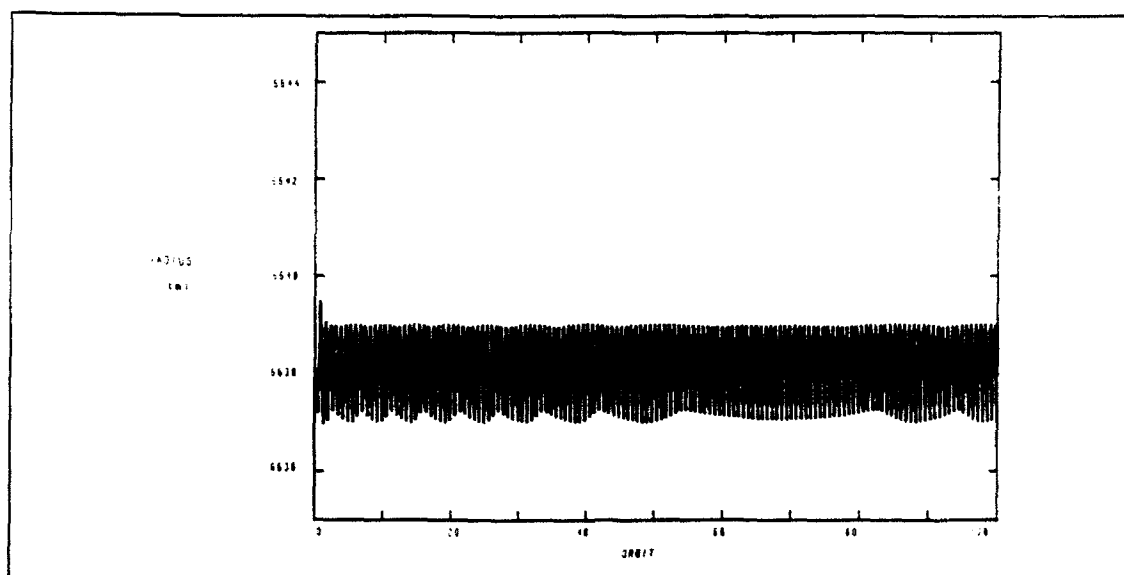


Figure 4 $\alpha=75^\circ$

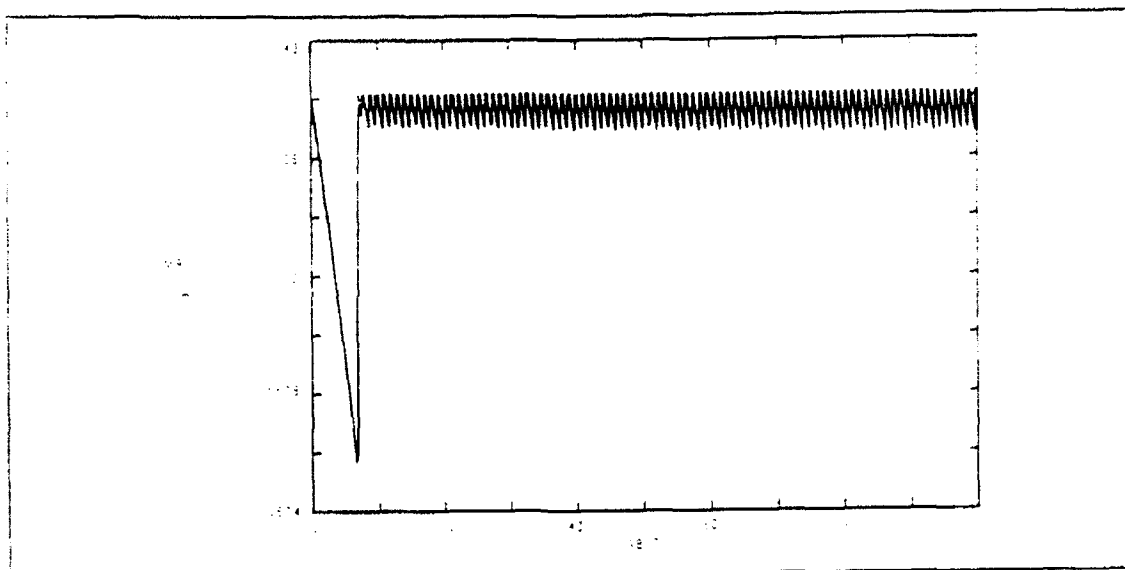


Figure 5 $\alpha=70^\circ$

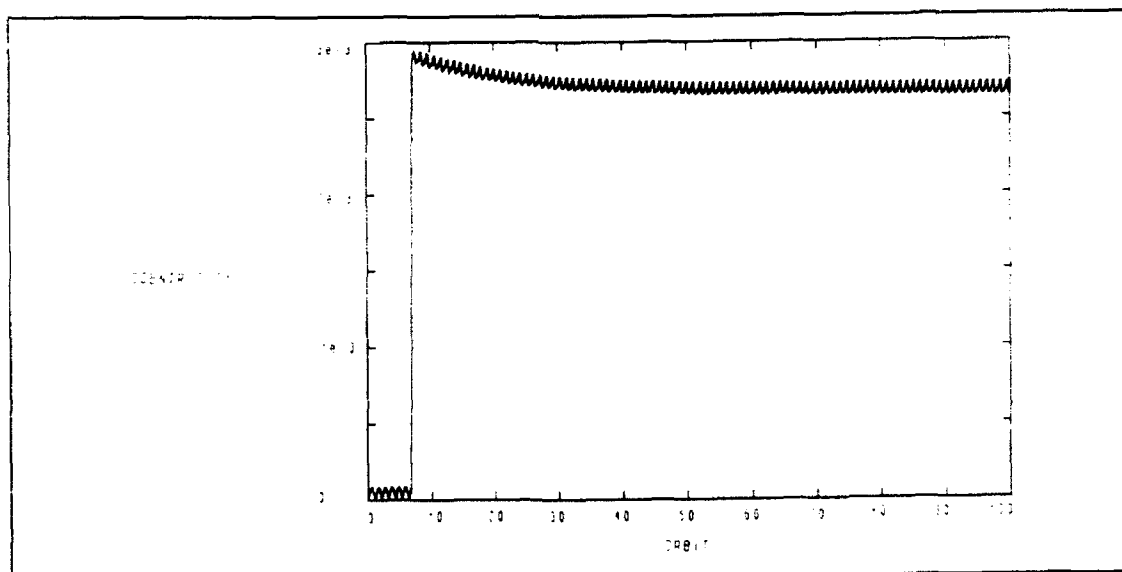


Figure 6 $\alpha=70^\circ$

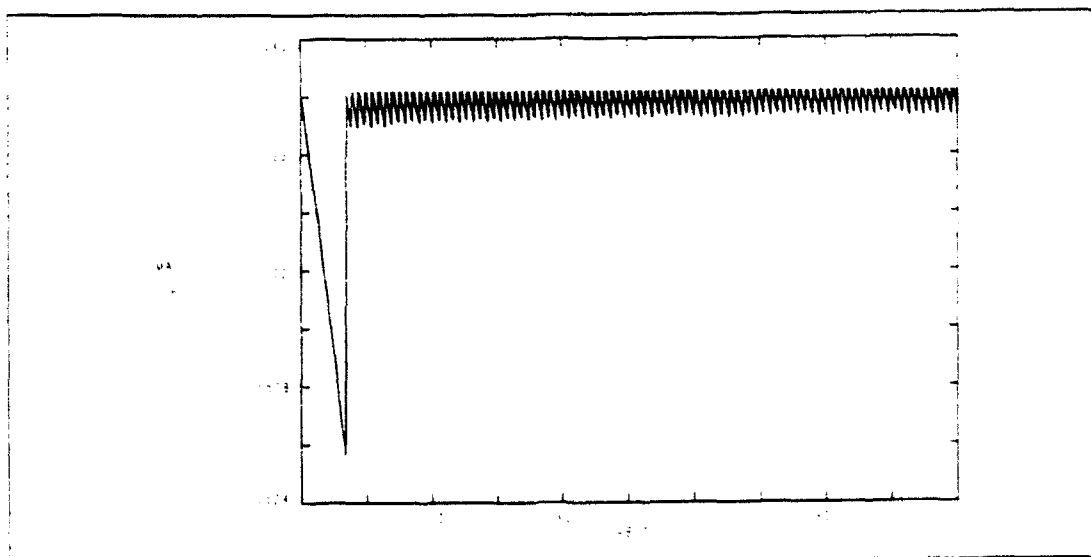


Figure 7 $\alpha=50^\circ$

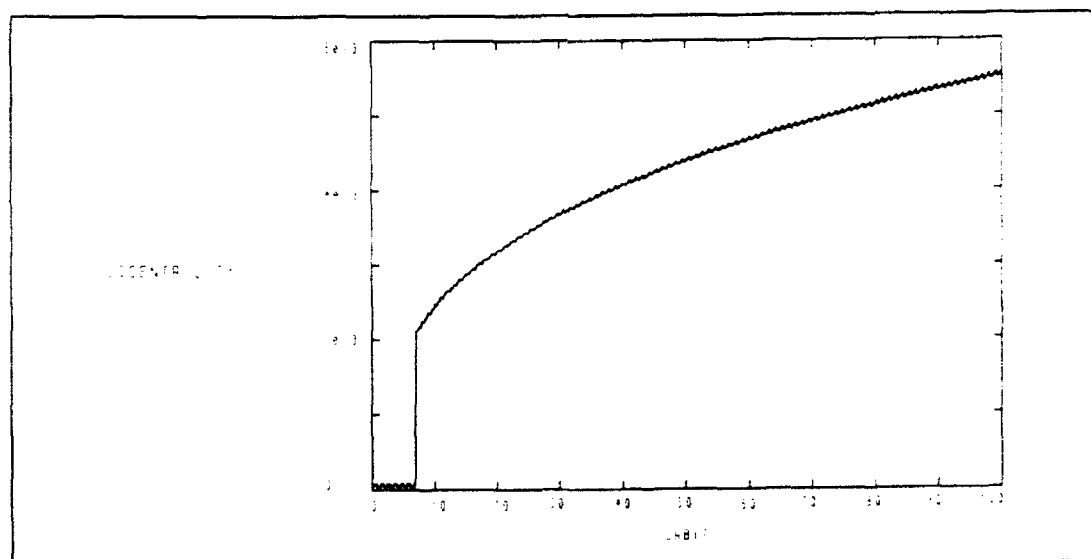


Figure 8 $\alpha=50^\circ$

APPENDIX E

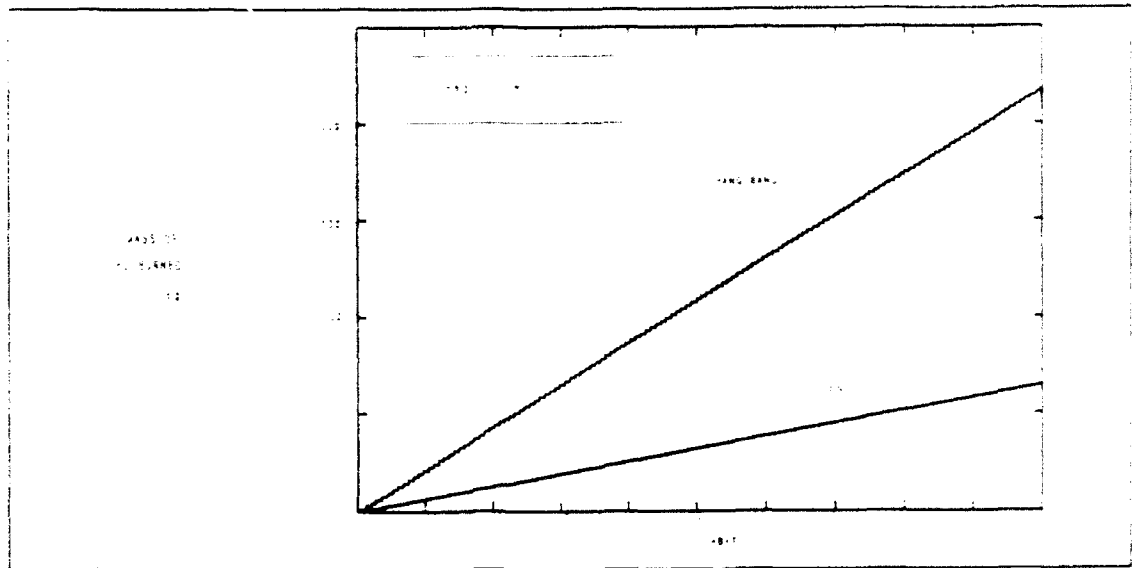


Figure 1

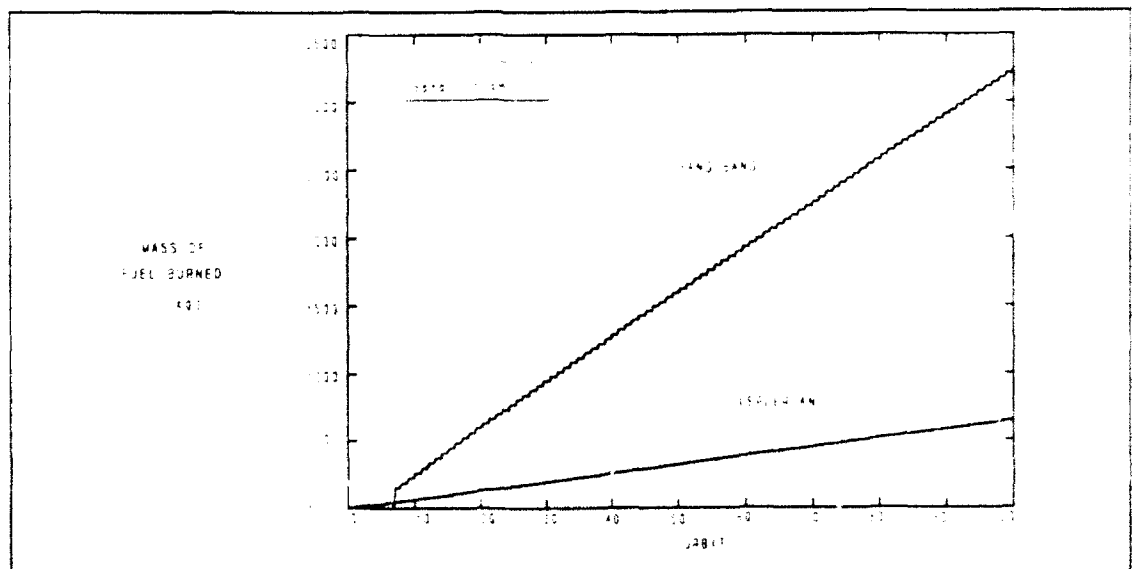


Figure 2

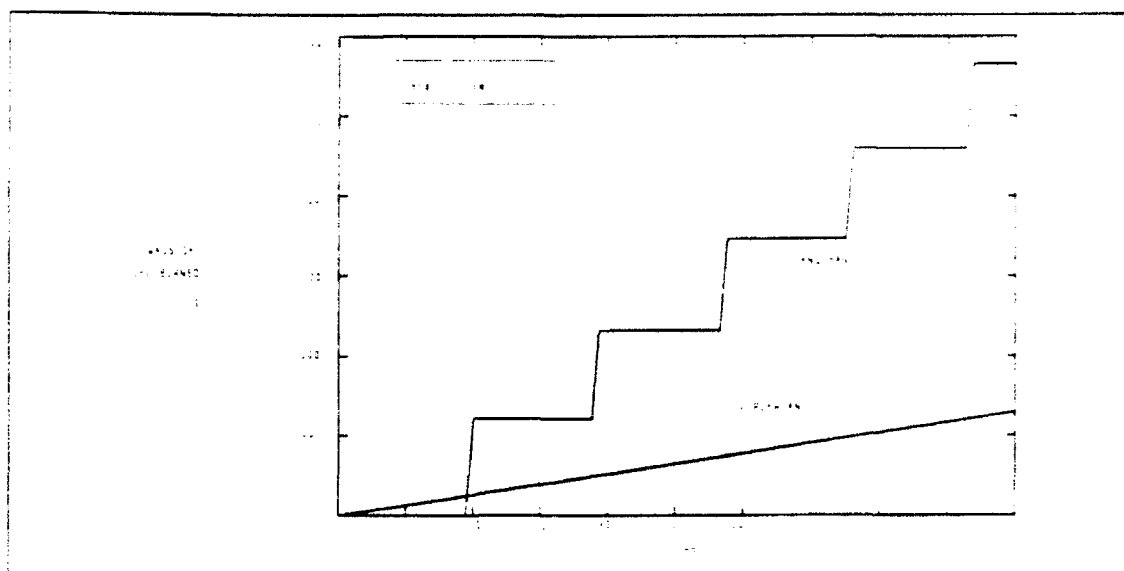


Figure 3

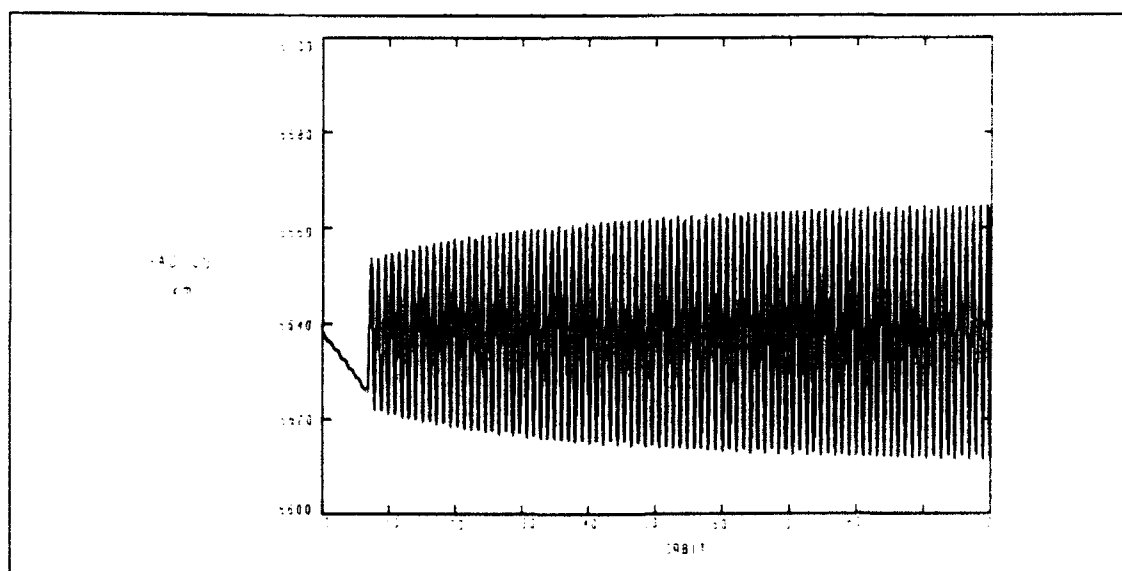


Figure 4 $\alpha=60^\circ$

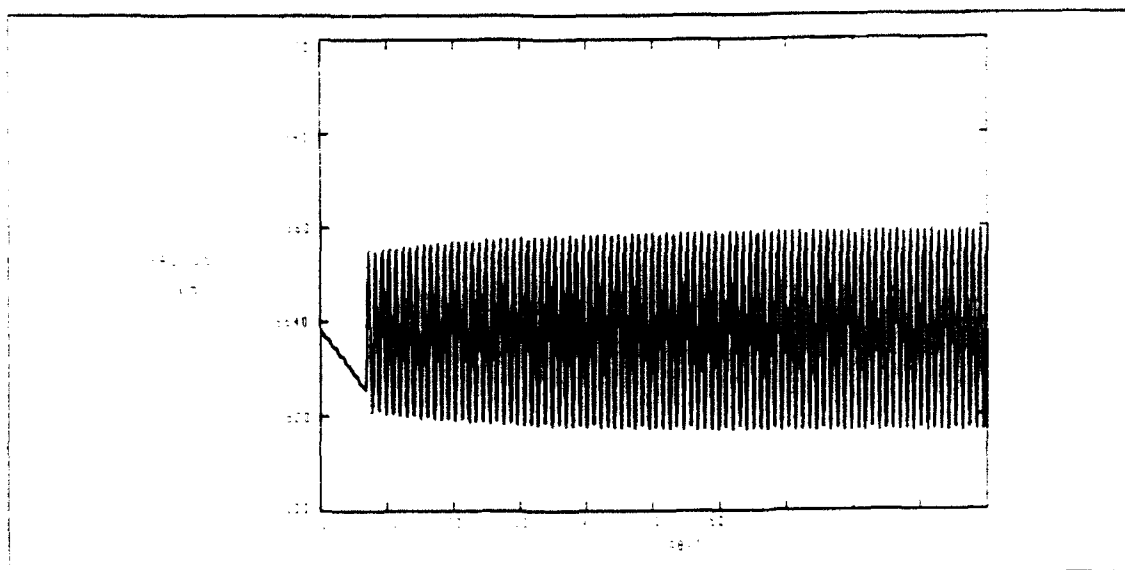


Figure 5 $\alpha=65^\circ$

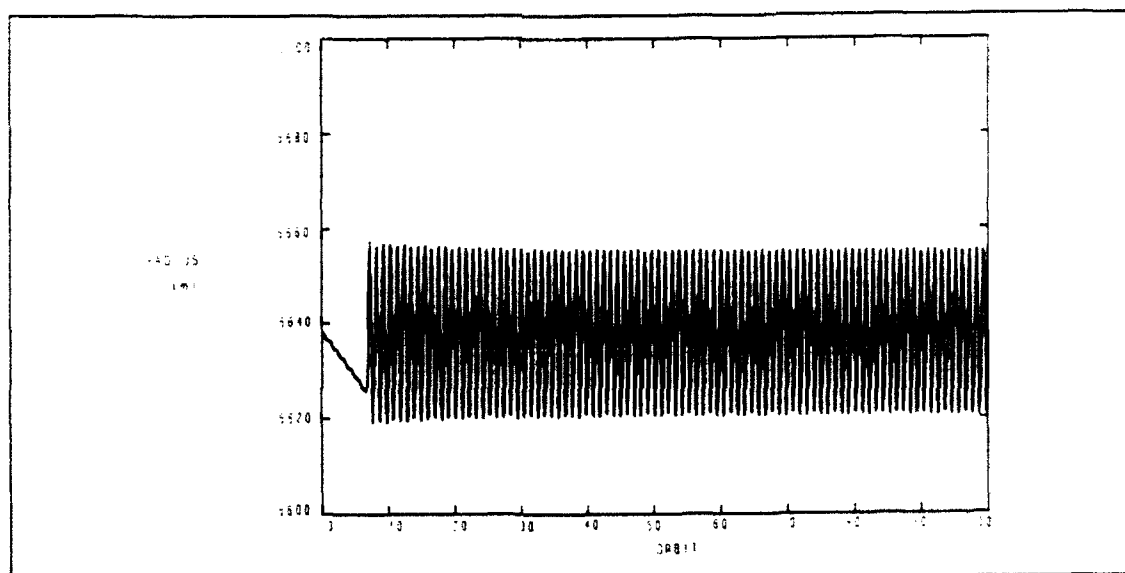


Figure 6 $\alpha=70^\circ$

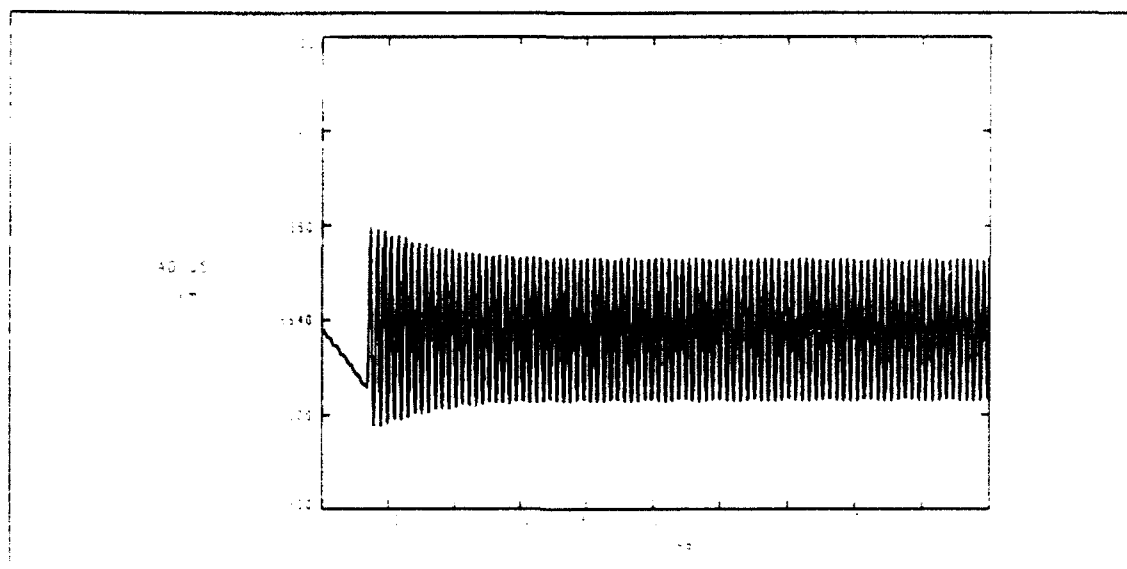


Figure 7 $\alpha=75^\circ$

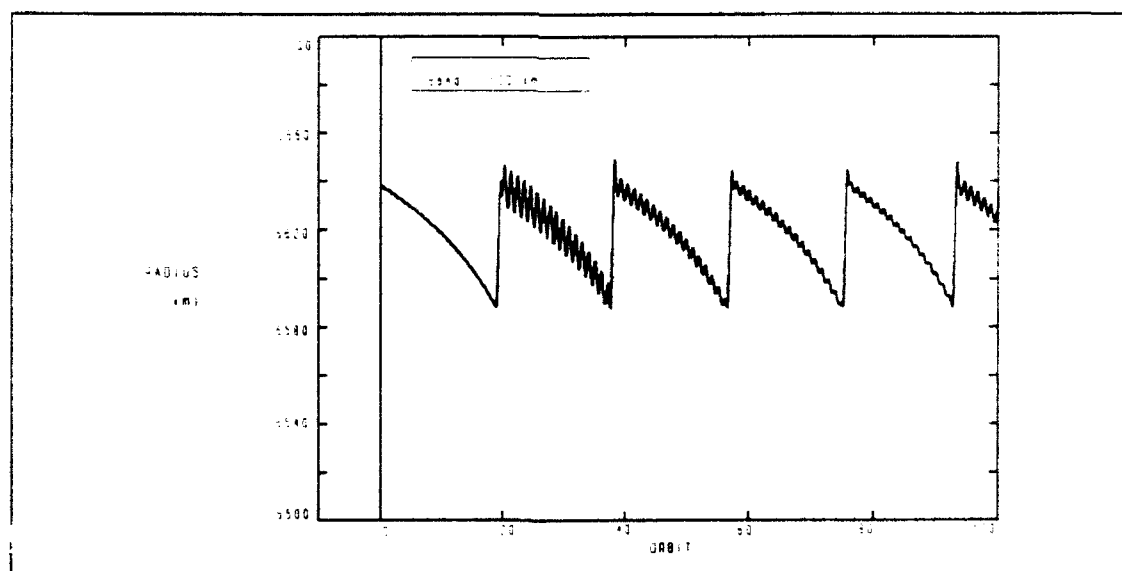


Figure 8 $\alpha=70^\circ$

APPENDIX F

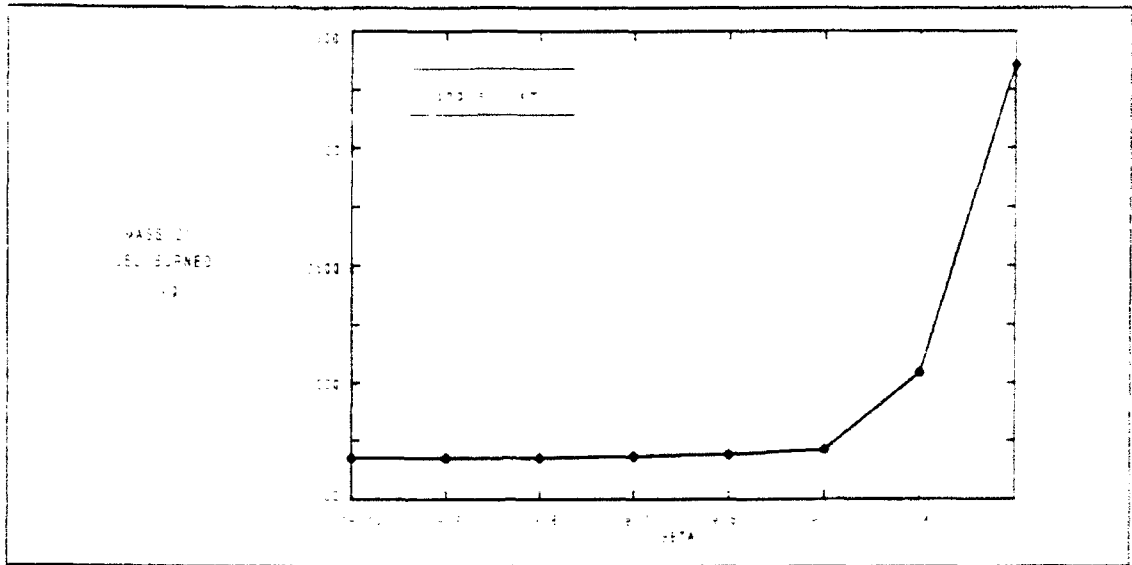


Figure 1

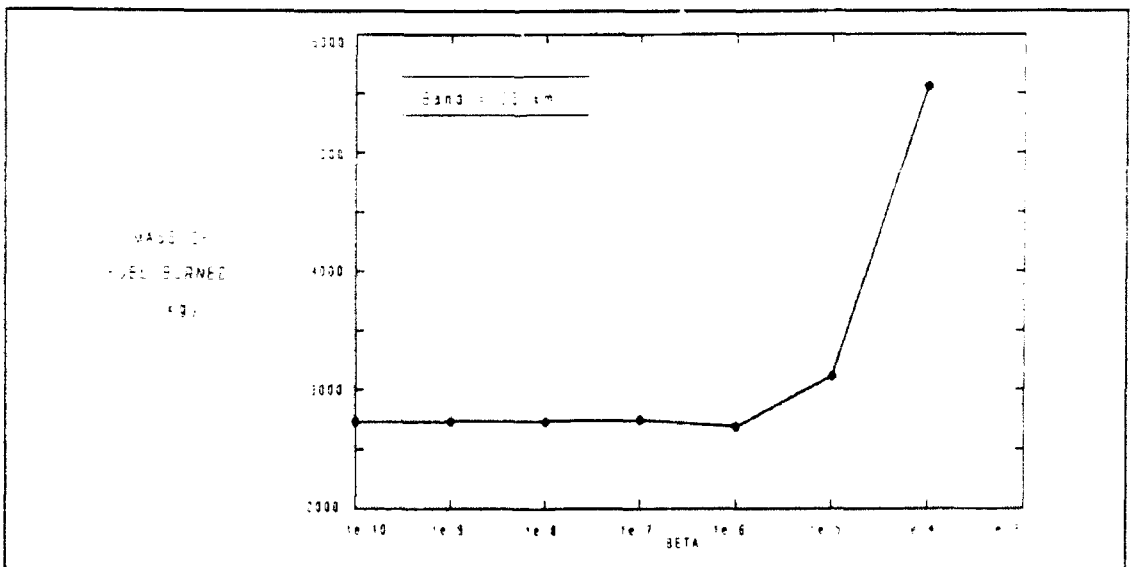


Figure 2

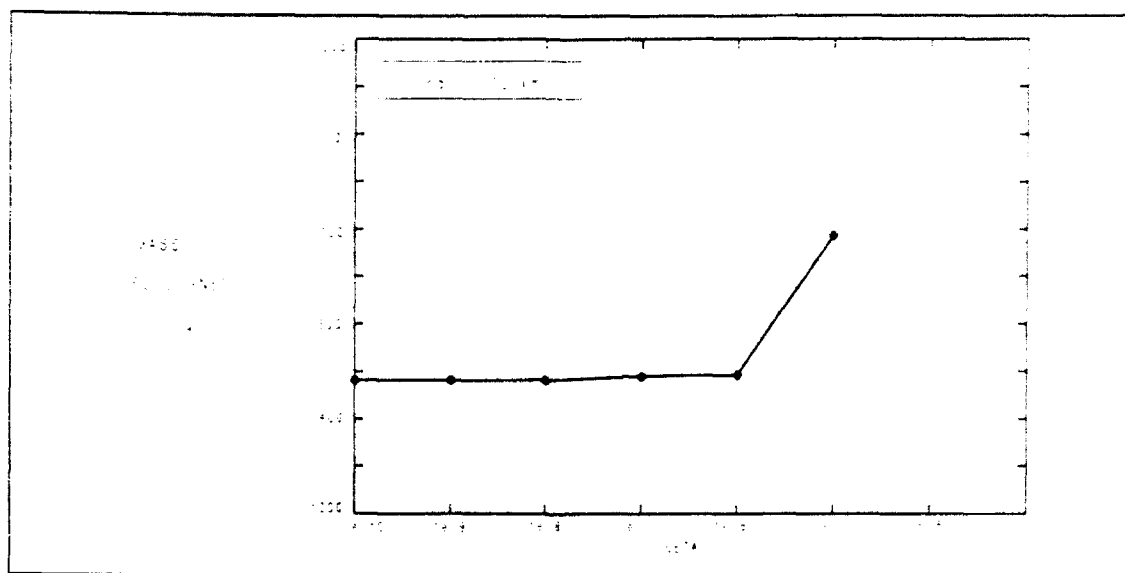


Figure 3

APPENDIX G

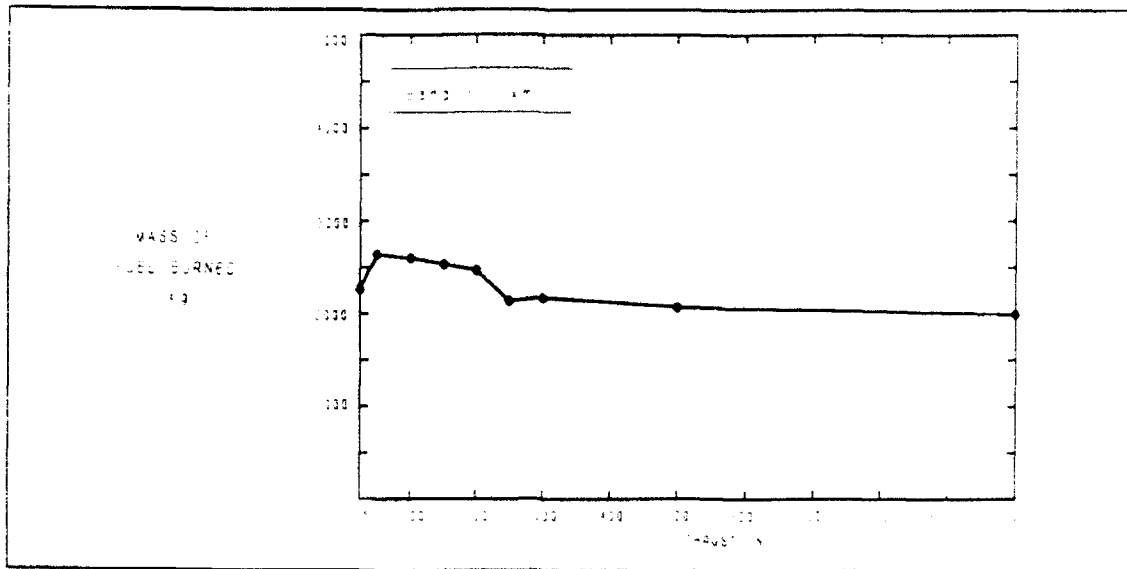


Figure 1

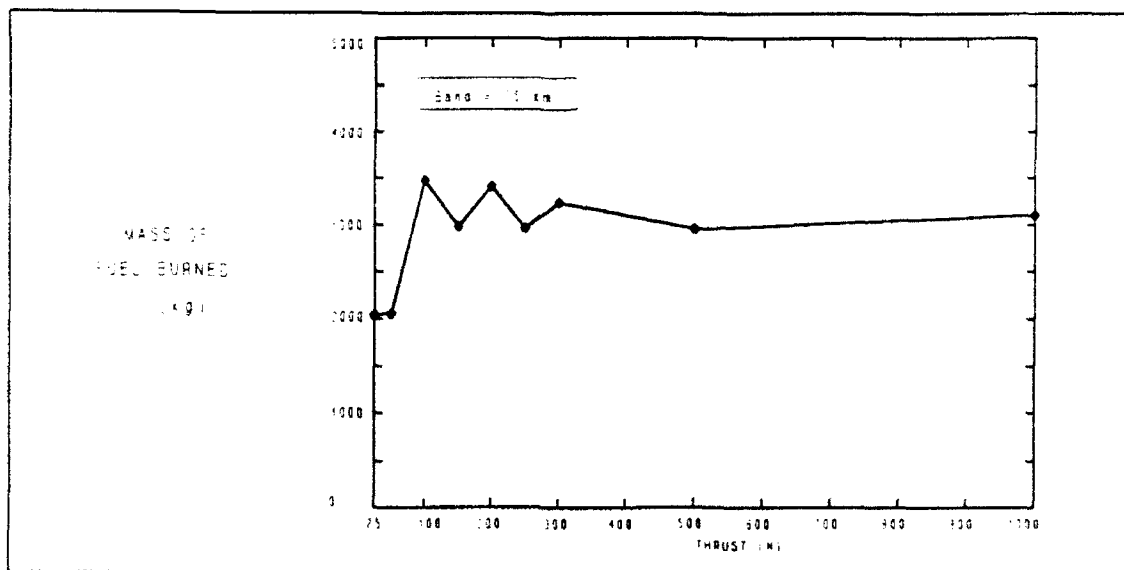


Figure 2

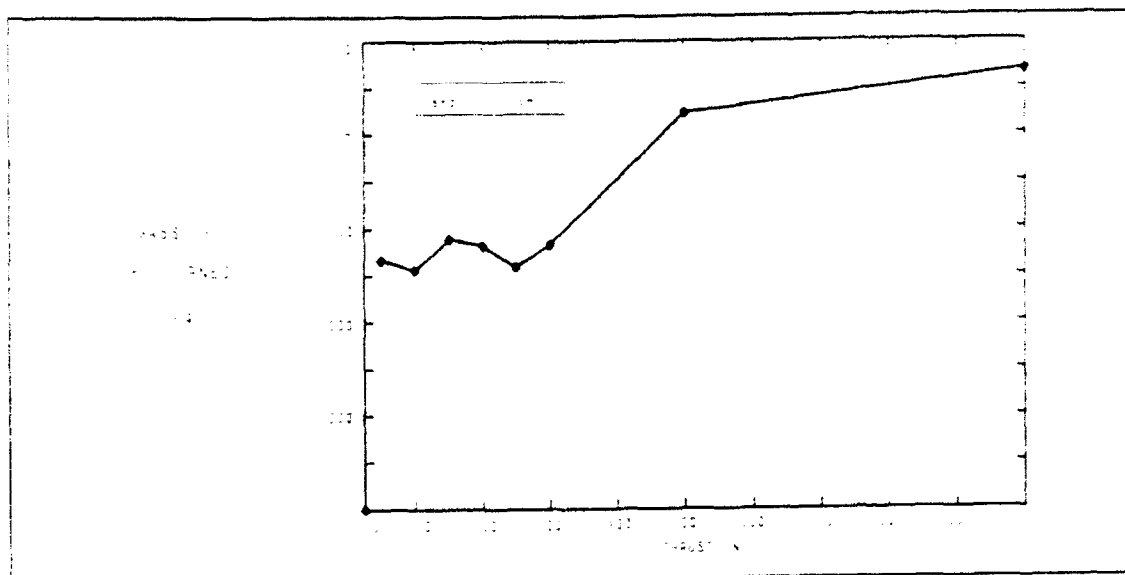


Figure 3

APPENDIX H

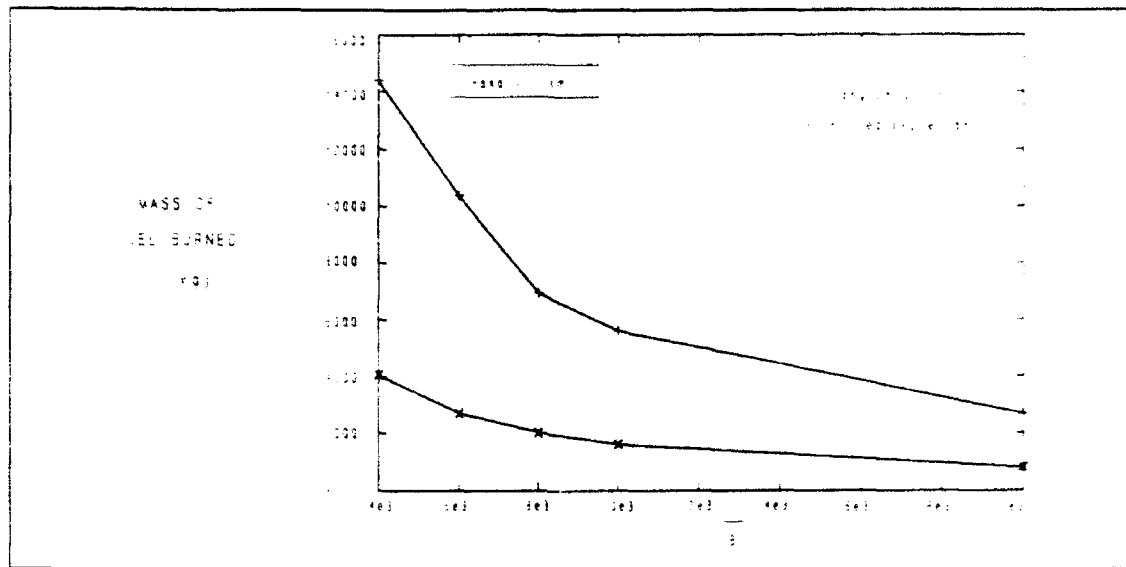


Figure 1

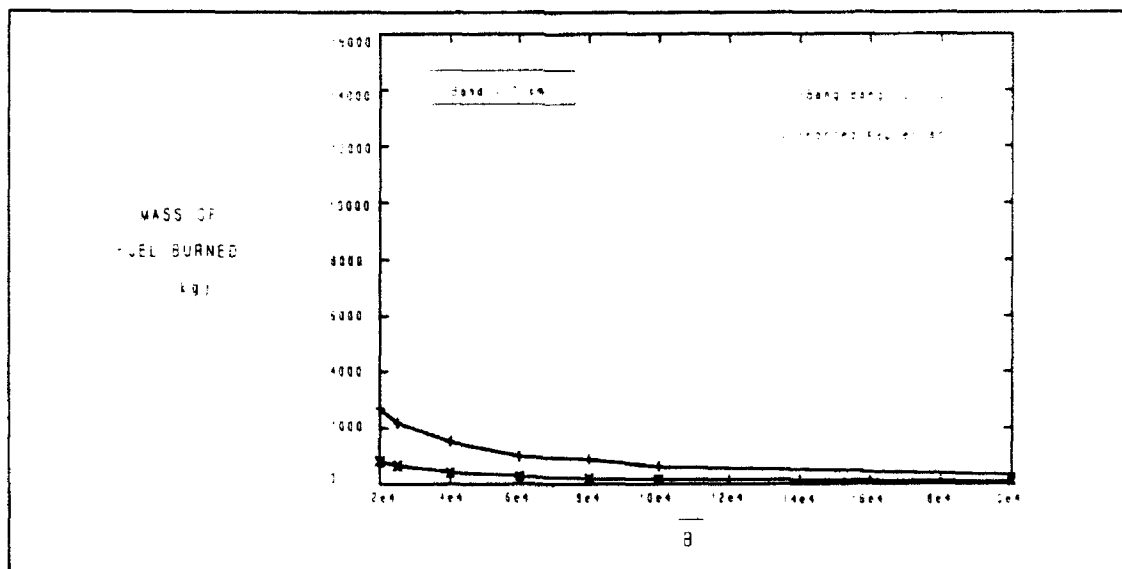


Figure 2

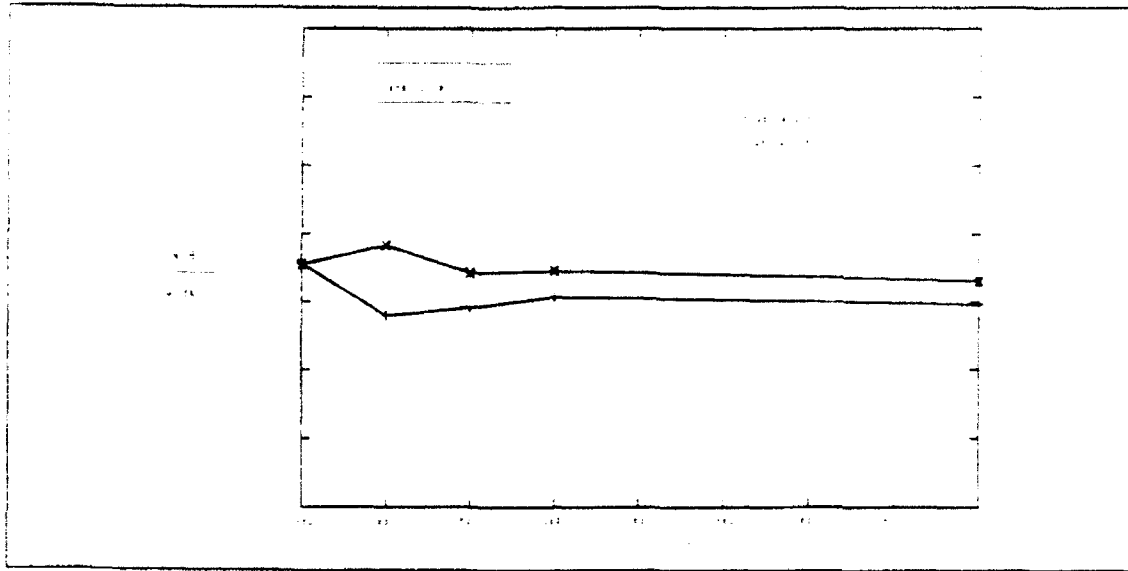


Figure 3

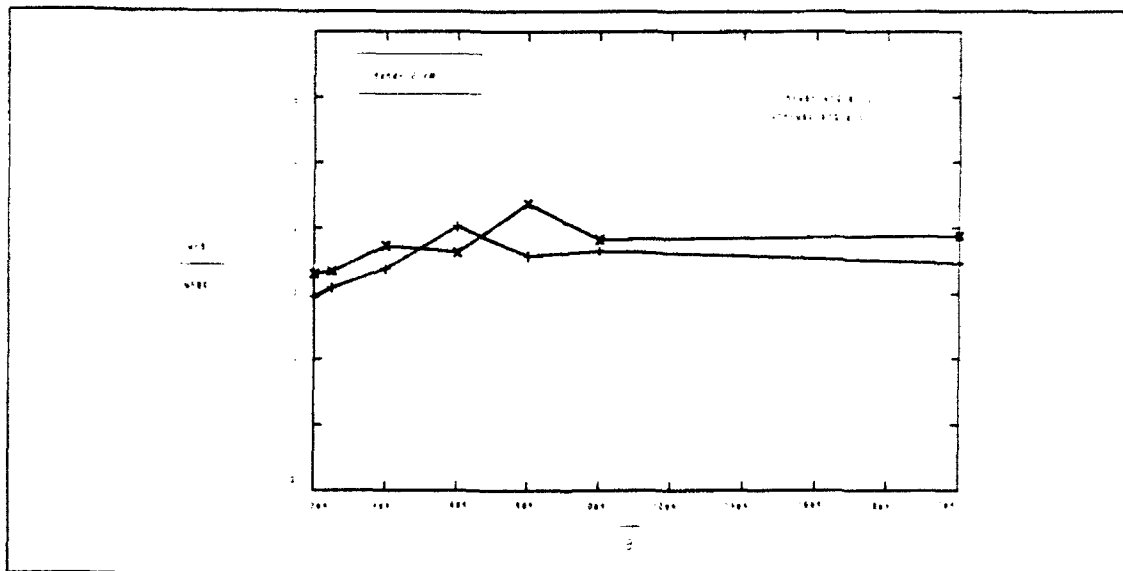


Figure 4

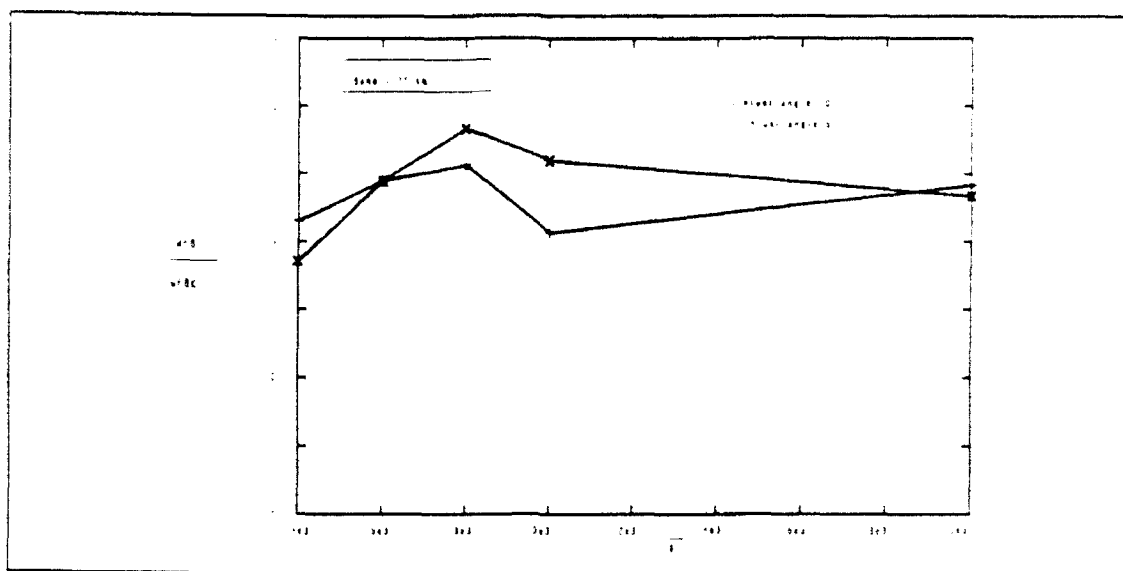


Figure 5

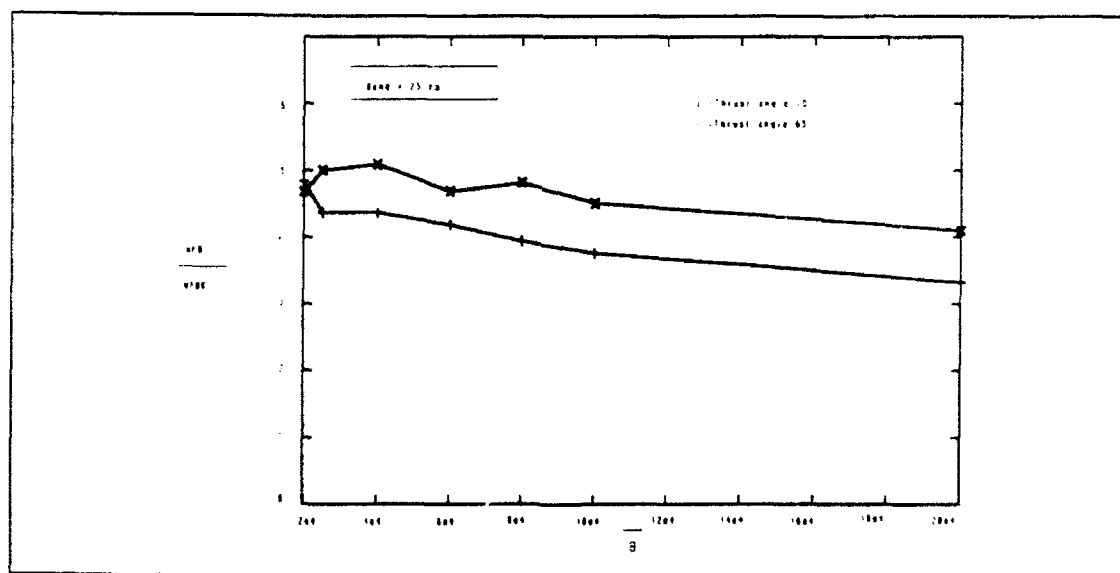


Figure 6

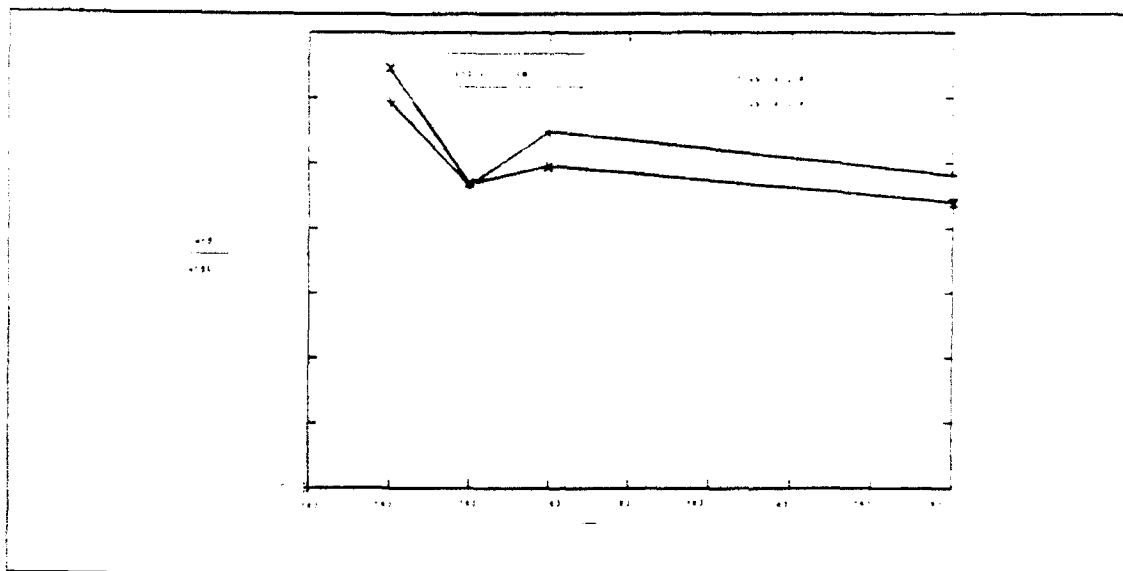


Figure 7

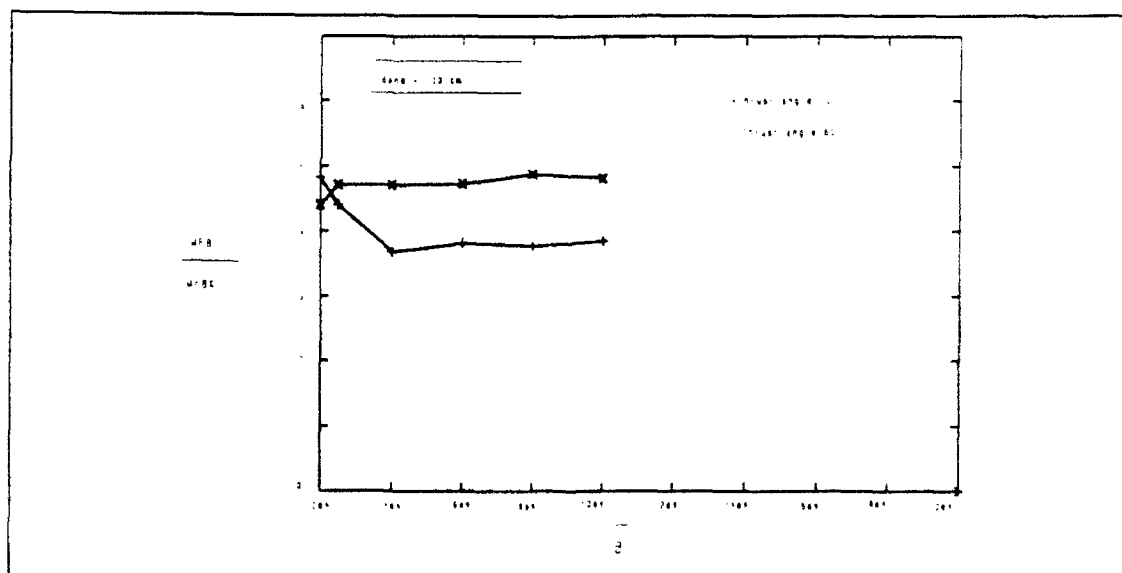


Figure 8

LIST OF REFERENCES

1. Kaplan, Marshall H., *Modern Spacecraft Dynamics & Control*, John Wiley & Sons, 1976.
2. Pauls, D. D., *Orbital Maintenance of Exoatmospheric Low Earth-Orbiting Satellites*, Master's Thesis, Naval Postgraduate School, Monterey, California, December 1991.
3. Ross, I. M. and Melton, R. G., *Singular Arcs For Blunt Endoatmospheric Vehicles*, Proceedings of the AIAA/AAS Astrodynamics Conference, Portland, Oregon, August 20-22, 1990, AIAA Paper # 90-2974.
4. Wertz, J.R. and Larson, W.J. (Eds), *Space Mission and Analysis Design*, Kluwer Academic Publishers, 1991.

INITIAL DISTRIDUTION LIST

- | | | |
|----|--------------------------------------------------------------------------------------------|---|
| 1. | Defense Technical Information Center
Cameron Station
Alexandria, Virginia 22304-6145 | 1 |
| 2. | Library, Code 52
Naval Postgraduate School
Monterey, California 93943-5002 | 1 |
| 3. | I.M. Ross, Code AA/Ro
Naval Postgraduate School
Monterey, California 93943-5000 | 2 |
| 4. | Brij Agrawal, Code AA/Ag
Naval Postgraduate School
Monterey, California 93943-5000 | 1 |
| 5. | Mark Wilsey
306 Greenpoint Ave
Liverpool, New York 13088 | 1 |